SIMULATION BASED DIMENSIONLESS WATERFLOOD PERFORMANCE CURVES FOR PREDICTING RECOVERY

By

Michael D. Dunn

RECOMMENDED:

Advisory Committee Chair

Department Head

APPROVED:

Director, School of Mineral Engineering

Dean of Graduate School

9-5-00

Date

SIMULATION BASED DIMENSIONLESS WATERFLOOD PERFORMANCE CURVES FOR PREDICTING RECOVERY

A

THESIS

Presented to the Faculty

Of the University of Alaska Fairbanks

in Partial Fulfillment of the Requirements

for the Degree of

MASTER OF SCIENCE

By

Michael David Dunn, B.S., M.S.

Fairbanks, Alaska

August 2000

ABSTRACT

Predicting waterflood recovery with simulation based dimensionless performance curves has advantages over the more traditional approaches in certain applications. This work discusses the advantages of the type curve approach in moderately mature fields where high resolution history matches are required. The method also has advantages when uncertainty analyses is important.

The dimensionless type curve methodology can be applied to many different fields. A case study of a large, complex field is presented to show how the curves are created and how they can be applied. In this field, a study of the geology and stratigraphy indicated that reservoir continuity, permeability variance, and effects of faulting were the most important drivers of recovery efficiency. Simulations were performed on 45 datasets to describe waterflood performance over the range of variation. A spreadsheet program was created to predict recovery of any description, based on interpolations of the simulation results.

The dimensionless curves can be used to predict full-field performance, as the basis of an integrated evaluation tool, and/or for comparing actual performance to predicted performance. Using correlations to predict recoveries allows for ease of sensitivity analyses, and ease of application by casual users in an organization.

TABLE OF CONTENTS

LIST OF TABLES

LIST OF FIGURES

AKNOWLEDGEMENTS

After 18 years in the petroleum industry, I am thankful to many who have helped me achieve my professional and academic goals. First, I would like to thank my Advisor, Dr. Godwin Chukwu, for introducing me to the M.S. Petroleum Engineering program at UAF. The work that he has done not only for me, but all the professionals in Anchorage, has made a significant impact on the oil industry in Alaska. I would also like to thank him for all the support and guidance he provided while developing this thesis.

I would like to thank Dr. David Ogbe, Dr. Vidyadhar Kamath, and Dr. Santanu Khataniar for serving on my committee and providing valuable advice. I would also like to thank the other professors who have served the Anchorage petroleum community.

The other individuals I would like to thank are too numerous to name, but are those ARCO colleagues I have worked with in Texas and Alaska. As the ARCO story comes to an end, I salute those individuals who through their commitment to technical excellence, made ARCO a great company.

Finally, I would like to thank ARCO Alaska, Inc. for providing the resources that made this work possible.

MDD, April 2000

CHAPTER 1

INTRODUCTION

Predicting hydrocarbon recovery using numerical simulation is a complicated and time consuming process. To adequately replicate the physical world with a numerical model, the geoscientists and reservoir engineers must have a solid understanding of the geology, reservoir, and fluid flow fundamentals. This demands a certain level of experience and expertise that is difficult to master. In addition, the time it takes to build the description, history match with actual data, and tune the model, can be particularly burdensome on an organization.

A case in point is a very large field on the North Slope. This field is embarking upon a massive re-development program to fully exploit the remaining reserves. Once considered a marginal oilfield, this field is now a leading contender for investment capital by all owners of the field. An issue that may prevent the full exploitation of this field is the reservoir forecasting capability necessary to test various development schemes and depletion strategies. Early in the life of this field, a full-field finite difference model was used to help size facilities and design drilling programs. Those decisions resulted in the building of three central processing facilities with gas lift facilities and a line drive drilling program on 160 acre well spacing. Today, the owners are finding that the existing facilities and the current well spacing are inadequate to fully maximize the field's productivity and future profitability.

Dozens of man-years have gone into enhancing and fine tuning the full-field model to achieve an acceptable history match so that correct decisions can be made based on predictive runs. Relative permeabilities have been tweaked, fault seal characteristics have been adjusted, layers have been added, but all to no avail. At this time, there is no acceptable history match and there appears to be little chance of achieving one. Reasons for the failure of an adequate history match are numerous. First, the field is huge. On an areal extent basis, it is one of the largest full-field pattern waterfloods in the world. Second, the stratigraphy and geology is extremely complex. Third, there are a number of recovery mechanisms, including miscible gas flood, which complicate the input and slow the computational time.

The shear size of the field is a significant impediment to achieving an adequate history match. The field covers an area of 100,000 acres with net pays ranging from 10 feet to 160 feet. To achieve tolerable turn-around times, the grid blocks had to be 8 acres or larger and only 8 layers

were used to describe the stratigraphy. Even with 8 acre grid blocks, the model took 14 hours to run a history match on an IBM RS6000 machine and 30 hours for a predictive run.

In mature areas of the field, the extrapolation of production data has been successfully used to predict pattern recovery. Employing a technique that relies on extrapolations of production performance, rather than simulations, is consistent with methods used in many mature fields. "Decline Curves" as they are often referred to, are a common technique of predicting future well performance under primary depletion as well as waterflood. At this field, the "cut-cum" or "log WOR"[1,2,3] technique has proven to be particularly applicable, and accurate, in mature patterns. In this context, "mature patterns" are those patterns that have established a straight line trend of log WOR (water-oil-ratio) versus cumulative production, which is usually evident at or above a WOR of 1.

For less mature patterns and in the miscible flooded areas, log WOR extrapolations are less applicable. These patterns have not produced enough water to establish a reliable WOR trend, or the miscible flood process has caused a shift in the trend. It is these patterns that can best benefit from simulation based type curves. In this context, a type curve is defined as a dimensionless curve (such as percent recovery versus hydrocarbon pore volume injected, or WOR versus percent recovery) generated from a finite difference pattern simulation that can be scaled to any size pattern.

The objective of this work is to highlight where this method is most applicable and develop a procedure for developing the dimensionless relationships. As part of the case study, a series of pattern level simulations are performed over a wide range of reservoir descriptions and pattern geometries. The results of the simulations are normalized on a hydrocarbon pore volume basis so that they can be applied to any size pattern. Finally, a spreadsheet-based program stores the dimensionless curves and allows the user to predict recovery and water cut behavior for any given description, and compare recoveries for a range of descriptions.

Three uses of the dimensionless curves will be discussed. The first is comparing actual well data to predictions by overlaying dimensionless production data over the dimensionless type curves. The second is using recovery curves for all wells in the field to predict full-field performance. The third use is using the curves as the basis of an integrated evaluation tool.

CHAPTER 2

METHODS TO PREDICT RESERVOIR RECOVERY

The challenge of choosing a method to predict reservoir performance is how to predict recovery efficiency for a given set of rock and fluid properties, as well as the range of uncertainty around these properties, while at the same time honoring site specific knowledge. To find the best approach, three different methods are discussed: finite difference simulation, analytical equations, and simulation based dimensionless performance curves (type curves).

2.1 Finite Difference Simulation

Reservoir modeling with finite difference simulation would be considered the most sophisticated approach. It involves the application of a computer simulation program to the description of fluid flow in the reservoir. Many different disciplines including geoscientists, reservoir engineers, and production engineers contribute to the preparation of the input datasets. Most would agree that it provides the best answer, but it also requires the most effort.

Finite difference simulation involves describing the geology, rock properties, and fluid properties with sets of numerical data. The model is then divided up into discrete grids or cells where the fundamental reservoir engineering equations of Darcy flow and material balance are applied. The method is not only intensive from a data gathering standpoint, but is also intensive from a computational standpoint.

Finite difference simulation plays a critical role in reservoir management decision making. It is best suited for quantifying complex recovery mechanisms and accounting for the effects of reservoir heterogeneities. However, in cases where uncertainty analyses is required, or high-resolution history matches are required, full-field numerical simulation may not be the preferred approach. Even though a finite difference simulation method may yield the most technically correct "answer" for a given description, for organizational, technical, and value of information reasons, other approaches may be more suitable.

2.2 Analytical Solutions

A second approach to predict reservoir recovery is to use the analytical solutions that have been developed in the petroleum literature. Muskat[7], Pratts[7], Craig[9], Dykstra[10], Parsons[10], and others, have developed a number of equations describing reservoir performance for various patterns, rock properties, and fluid properties. However, the use of these analytical approaches is limited because of the simplifying assumptions about pattern shape (e.g. 5 spot vs. line drive), PVT properties (e.g. mobility ratio), and rock properties required to describe the performance with simple equations.

2.3 Dimensionless Type Curve Approach

A third approach might be considered a combination of the two methods discussed above. A pattern-level finite difference simulation is run for a range of rock properties, fluid properties, and/or pattern shapes. The output data from these simulation runs are normalized to a set of dimensionless curves such as log WOR versus percent recovery, or percent recovery versus hydrocarbon pore volume of water injected (HCPVWI). These "type curves" are used to describe the range of performance over the range of potential input for any size pattern or reservoir.

If the evaluator had complete confidence in a single point estimate for each and every variable, or very little production data were available, a single reservoir simulation could be used to predict performance. A major problem with this approach is it does not account for uncertainty. On the other hand, if the subject reservoir matched the descriptions that were the basis for the analytic equations, the input variables could be easily adjusted to see the effect of uncertainty on reservoir performance. However, if the reservoir is not homogeneous, as is assumed in most analytical solutions, and/or the pattern shapes do not fall into one of the standard categories, then the analytical approach may do a poor job of predicting recovery.

The dimensionless type curve approach, on the other hand, can account for the specific reservoir, fluid, and pattern shape complexities of the given reservoir. By normalizing production data, the simulation output (dimensionless curves) can be easily history matched. Also, because the performance is described with dimensionless curves that were previously created with a reservoir simulator, the time it takes to re-predict pattern performance for a different set of input variables is very quick. This makes it easy for the engineer to perform sensitivity analyses, and to generate a database of information that serves as the basis of integrated reservoir evaluation tools.

CHAPTER 3

CONSIDERATIONS WHEN CHOOSING A RECOVERY PREDICTION TECHNIQUE

When choosing a reservoir recovery prediction technique, there are two main sets of factors to consider in the decision. The first set of factors pertains to the stage of the subject oilfield's life. The second set pertains to organizational and technical issues that affect resource allocation decisions. A discussion of these factors is the subject of this chapter.

3.1 Stage of an Oilfield's Life

Shortly after a field is discovered, while major drilling and facility strategies are being formulated, the reservoir engineer has very little if any production data. The data that is available consists of a geological model derived from a sparse set of core and log data, and lab measurements of oil properties, rock properties, and saturation functions. At this stage in a field's life, the reservoir engineer has little choice in choosing a recovery prediction technique. He must rely on a method that uses rock and fluid data to "simulate" future production. If the field is simple and homogeneous, predictions of rates and recoveries can be made with analytical equations. More often than not, forecasts are made with a finite difference model to accurately honor the geological and fluid flow complexities of the reservoir in question.

At this early stage of a field's life, the types of development decisions that must be made require an understanding of the capacity of the reservoir in terms of total oil, water, and gas rates. Development engineers are attempting to size equipment such as separators, water injection pumps, and gas compressors to handle "expected" fluid rates. These types of decisions do not require precise predictions of well by well behavior in the future, but rather what the total field capacity is likely to be.

Later in the life of a waterflood, there are two major differences. First, there is plenty of field data that can be extrapolated to predict future water cut performance and ultimate recovery on a pattern by pattern basis. The validity of the log WOR technique has been documented in a number of studies[1-5]. The use of the log WOR decline curve technique is most useful during this phase. Secondly, the types of facility decisions that are being evaluated generally require more precise estimates of oil, water, and gas production. Facility expansions that are contemplated at

this stage are generally designed to allow production of wells that are shut-in because their GOR (gas-oil-ratio) or WOR (water-oil-ratio) is above the marginal cut-off.

During the moderately mature phase of a waterflood, some patterns have adequate data to extrapolate while others do not. It is this phase of a field's life when simulation based dimensionless curves can be used in conjunction with dimensionless production data to predict recovery of all patterns. The dimensionless type curve technique incorporates the best of both methods. It uses available rock and fluid property data to predict watercut behavior and recovery of a dimensionless pattern. The curve can then be displayed alongside normalized (log WOR versus percent recovery) production data. The result is a technique that allows for ease of history matching at the pattern level. As discussed in the next section, the ease of a history match by those individuals most familiar with the pattern, is an important advantage of this method.

Facility decisions in the moderately mature phase of a reservoir are often based on GOR and WOR wellsorts and how much oil can be produced with added fluid handling capacity. To illustrate the importance of predicting accurate "well sorts", Figures 1 and 2 are shown. These figures are based on a field on the North Slope of Alaska with actual simulator output and actual production data. Both curves are based on well-by-well data, sorted by GOR, where the solid black curve is output from the simulator and the lighter curve is the actual GOR sort for all wells in the field.

Each curve is plotted as cumulative oil production and cumulative gas production of all the wells, sorted by GOR in ascending order. The slope at each point is the GOR of that particular well in the sort. This field on the North Slope is undergoing not only pattern waterflood, but also gas injection in the form of immiscible and miscible injection. The wells near the bottom are those at solution GOR, where the wells near the top are the ones undergoing significant gas breakthrough.

The curves are presented in this manner because it is easy to see what the field is capable of delivering for a given gas handling capacity. In this case the gas injection capacity is 310 mmscfpd. It is not coincidental that the two curves cross at this point. In order to achieve a history match of total oil, water, and gas production rates, the simulation-based model was adjusted to match actual field production rate. As a result, the facility limited field production rate is about 257,000 bopd, which accurately matches the actual field production rate.

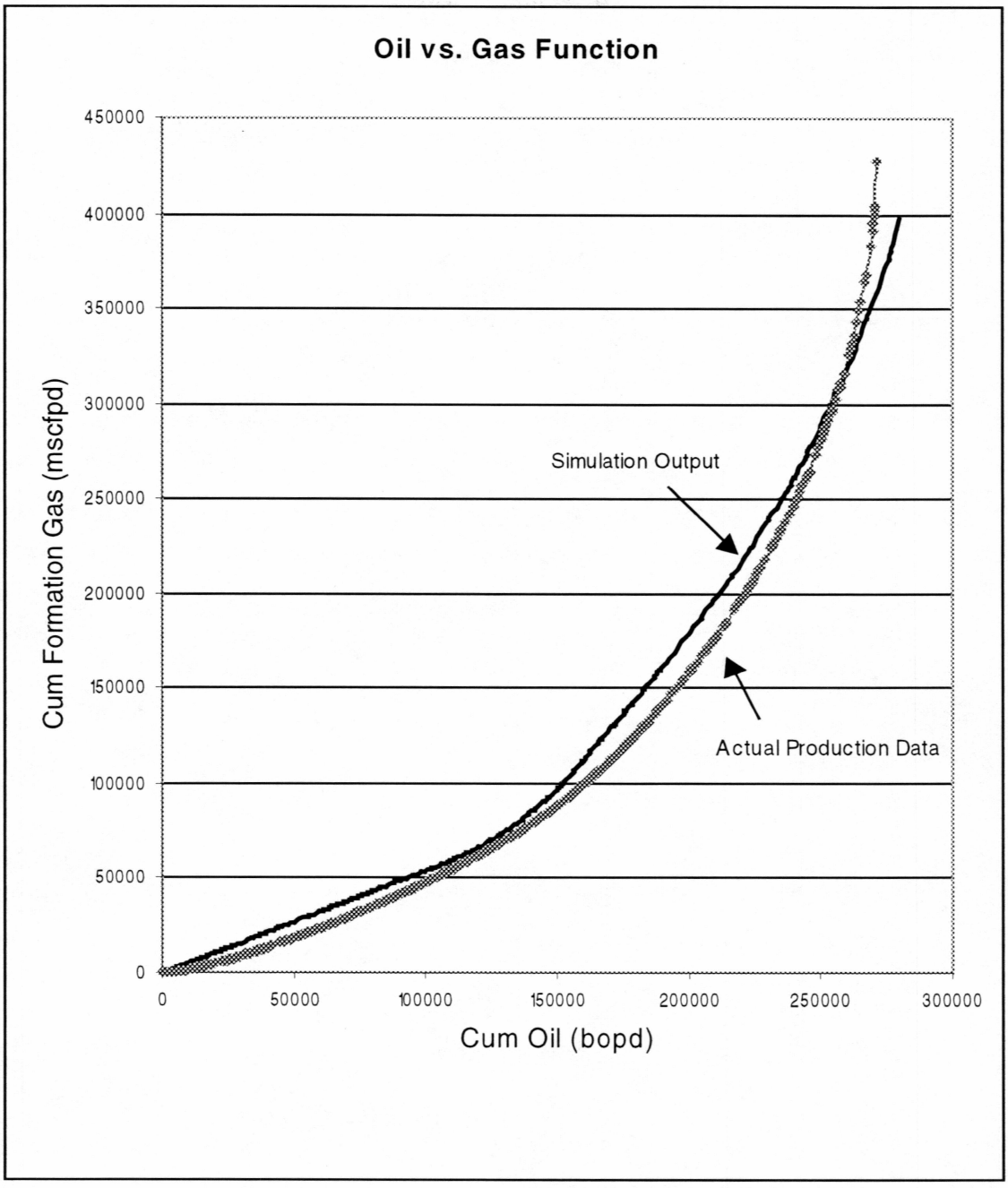

Figure 1: Comparison of Simulator Output to Actual Field Data

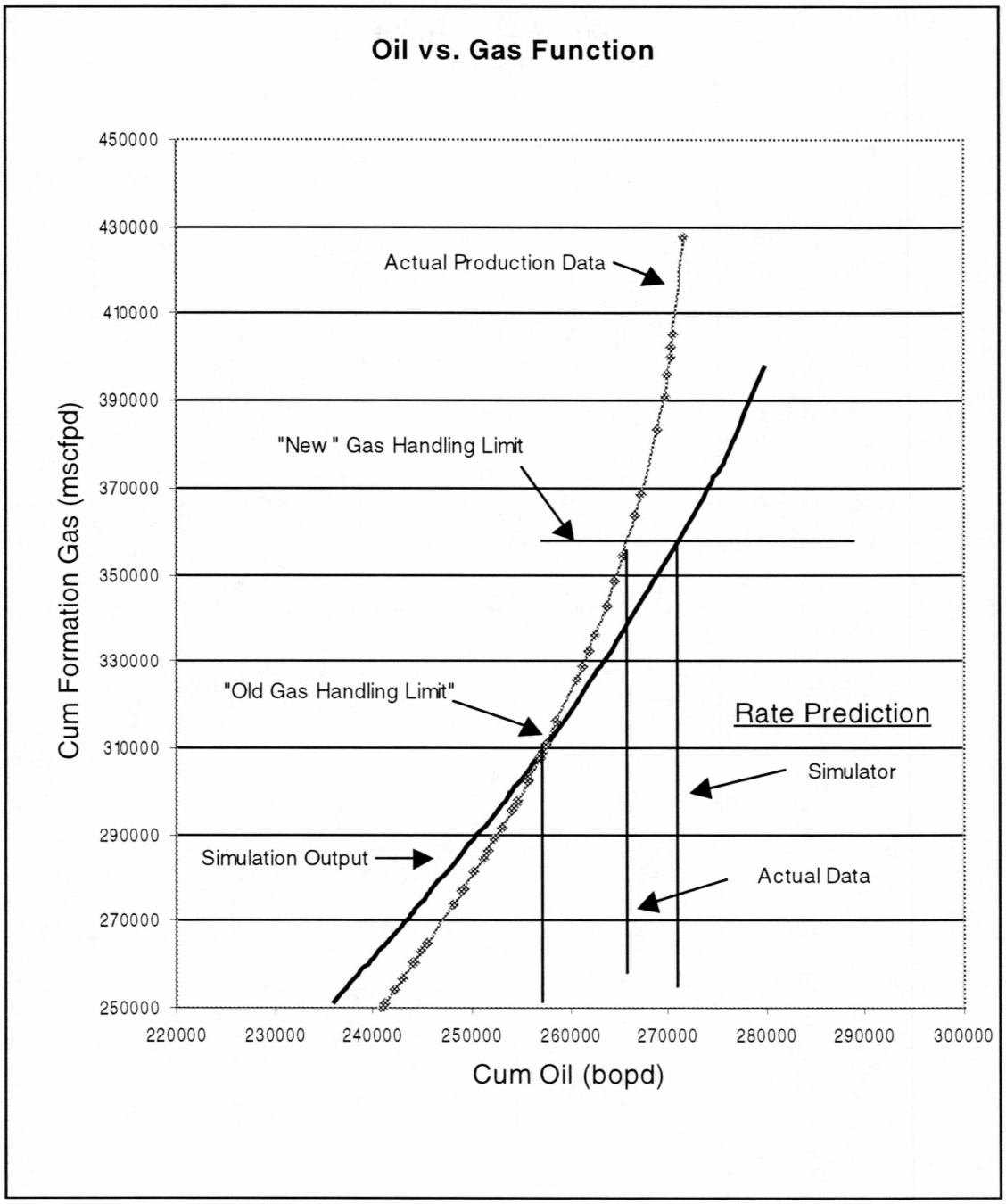

Figure 2: Impact of GOR sorts on prediction of oil rate impact from added gas handling

For many types of macro-strategy and budgeting decisions, this would be considered an acceptable history match. However, if the decision is whether to add gas compression, the simulator output significantly overstates the value. This is illustrated with Figure 2, which is a scaled-up version of the Figure 1 well sort near the top of the curves. If one were to predict the oil rate impact of adding 50 mmscfpd of gas compression (to 360 mmscfpd), the well sort from the simulator suggests the additional oil rate is close to 14000 bopd, where the actual well sort suggests the amount is closer to 9000 bopd. This makes it apparent that when faced with decisions that are designed to affect marginal producers, that the shape of the well sort is as important as the endpoints. This leads to the conclusion that a technique that accurately predicts pattern level performance is important when making decisions during the moderately mature stage of a field.

3.2 Organizational, Technical, and Value of Information Tradeoffs

When faced with the task of predicting reservoir recovery, we must also consider organizational issues, resource issues, technical issues, and the value of information. The objective of finding the best method, is to seek an optimal balance between all competing perspectives.

In terms of organizational issues, the preferred method should be one that engages all individuals that have knowledge that can affect future decisions. If future decisions are site specific in nature, such as where to drill infill locations, than a coarsely-gridded, full-field model may not be the preferred approach. In this example, a finer gridded model that honors the site specific knowledge of the geology and sealing nature of faults should be created to help pick drilling locations.

One of the shortcomings of full-field finite difference models in large organizations is that the local knowledge of a pattern (or well) may not be incorporated into the numerical model. This may be caused by two reasons. One, the numerical model may have had to be simplified to allow for acceptable computational times. These simplifications may take the form of coarse gridding and large cells, or simplistic correlations to describe complex behaviors such as miscible flooding. The second reason may be due to the inherent barriers to good communication in very large organizations. These organizational barriers prevent site-specific knowledge about the rock or fluid properties from being communicated to the model builders. For example, if a production engineer believes that a fault is sealing, unless he tells the model builder, his knowledge will be ignored if the geological model shows there to be sand-to-sand juxtaposition. Often times, he is

reluctant to make that simple phone call because the history match at the pattern level is so poor that he can not imagine how the full-field model will help him make decisions. The problem becomes one of the chicken and the egg. He is reluctant to contribute to the model definition because it serves no purpose, but it serves no purpose because the model does not incorporate site specific knowledge.

One way to insure site specific knowledge is incorporated into the model is to design a methodology that distributes the tasks of history matching to the individuals most familiar with their subset of data. This eliminates the need for communicating information from one group to another. It also encourages the surveillance engineer to look for reservoir reasons why a pattern is performing the way it is. Once the surveillance engineer has seen that his knowledge is incorporated into the model, he develops a sense of responsibility for the accuracy of its predictions. Once this is achieved, history matches at the pattern level become possible.

Another resource issue to consider is the manpower required to build and execute simulator models. Because of the expertise required to build accurate models, one can not expect every surveillance or production engineer in the organization to build "models". It is best to have a few highly qualified reservoir engineers build these models, but make sure that the results are distributed to the appropriate engineers and decision makers.

In terms of technical issues, most reservoir engineers would agree that a finely gridded finite difference simulation of the specific reservoir or pattern in question would be the best way to account for the unique features of that single description, and best predict "expected" reservoir performance. However, this method does not easily allow for certain types of sensitivity and uncertainty analyses.

For example, a decision maker may be interested in how the value of a decision changes if the reservoir is different than expected. A typical question that management may ask regarding a drilling location, may be: "what if the initial water cut is 50% instead of 20% as you have predicted"? These type questions stem from past predictions and past performance. For instance, the last well that was proposed may have had an expected rate of return of 20% if the initial water cut of the well were 30%. The well was drilled but it produced at much higher than expected water cuts. In hindsight, the well delivers a rate of return of a marginal 10%. When this happens, the decision maker is interested in the effect of similar surprises in future proposals.

To answer these types of simple questions with a numerical model, the engineer would have to adjust the geologic description to match a specified water cut at a specified location. He might for example add a thief layer, or change the sealing characteristic of nearby fault, or delete a fault altogether. This process can be very time consuming. On the other hand, if the point on a recovery curve or the size of the pattern can be changed to match the hypothetical outcome proposed by management, the answer to management's question can be arrived at very quickly. This is a suitable approach when addressing the value impacts of hypothetical situations and for screening the effect of uncertainties. It does not necessarily contribute to a better understanding of reservoir performance.

Another example of a sensitivity analysis that may be difficult to perform with a simulation based model is one involving optimal facility sizes. Many simulators have the facility logic tied directly to the reservoir model to estimate a "facility limited oil rate" at each time step. If this is the case, and the computational time to make a predictive run is measured in days, the time required to run 4 or 5 sensitivities on gas compression capacity may require a week or more of computational time. With turnaround times of this length, a comprehensive sensitivity analyses to find "optimal" facility sizes may not be performed as often as it should.

In terms of value of information[6], the simple fact is that reservoir forecasts or models do not by themselves make oil or money. The model's only purpose is to help make decisions that eventually lead to more oil production. One problem with "black box" simulators that yield a facility limited oil rate stream, is that the relationship between what can be affected by investment level, and what is a function of mother nature, can be difficult to interpret. For example, suppose a surveillance engineer was faced with the question of whether to spend money on infill wells, or spend money on electric submersible pumps (ESPs) to increase drawdown at the producers. Supposed both projects have the same present worth, are they equivalent projects? Probably not, because the infill drilling option is exposed to more reservoir uncertainty. The infill option is exposed to changing the pattern geometry and perhaps exposed to more reservoir continuity at tighter well spacing. These relationships are easier to understand if recovery efficiency and throughput rate are treated separately.

3.3 Advantages of the Simulation Based Dimensionless Type Curve Approach

The following bullets summarize the advantages of the dimensionless type curve approach:

- This approach limits the finite difference modeling to a few, qualified reservoir engineers, but allows results to be used by any and all users.
- The range of input data used for the simulations can account for the unique features of each pattern, without the need for oversimplifications.
- Once the stratigraphic, geologic, and reservoir parameters that affect recovery are identified, the history match can be performed by the engineer or geologist that is most familiar with their subset of data. Once this participation is achieved, full-field history matches at the pattern level become possible.
- Predicting recovery with type curves is fast, allowing for sensitivity and uncertainty analyses.
- Recovery and throughput are de-coupled. Since recovery efficiency is largely dependent on the reservoir description and throughput is largely dependent on the investment level, the relationships that affect the value of information calculation become more evident.

CHAPTER 4

GENERATING DIMENSIONLESS PERFORMANCE CURVES

To create and use dimensionless type curves, the geologist and reservoir engineer must decide which input variables have the greatest impact on reservoir performance so that simulation sensitivities on these variables can be run. A list of factors that can affect waterflood performance is shown below. It is noted here that this is only a partial list, as the factors affecting performance are highly dependent on the reservoir in question.

1. Pattern shape – symmetrical, balanced shapes are more efficient than asymmetrical or skewed shapes.
2. Permeability Variation – a reservoir that has layers of very high permeability and very low permeability will have less recovery at a given WOR cutoff than a reservoir with little permeability variation.
3. Oil Viscosity – a reservoir that has oil with a high viscosity (unfavorable mobility ratio) will recover less oil for a given volume of water injected than the same reservoir with low viscosity oil.
4. Wettability – Depending on rock properties such as pore throat size, an oil wet rock will usually recover less oil than a water wet rock.
5. Continuity – A reservoir with layers that are discontinuous at interwell distances will have less recovery than a reservoir that has high continuity.
6. Faulting – The more faulting, the more skew, the less efficient the waterflood. Faults can be barriers, channels, or conduits that tend to cause early water breakthrough.

It is recommended that the user choose the 3 or 4 most important factors that affect recovery efficiency, and try to describe the range of variation with 3 or 4 input variables in each set. Any more than this and the number of simulations required to create all the dimensionless curves becomes a bit unwieldy. For example, selecting 3 different factors and 3 different input variables for each factor would require 27 different simulations to generate the dimensionless type curves.

Once the primary factors have been identified and the range of variation is described with distinct values or relationships (e.g. relative permeability curves), the reservoir engineer must create a reservoir simulation dataset for each case and run the simulations. It should be noted that only

the variables that significantly affect waterflood performance, as defined for example by percent recovery at a given WOR (i.e. 30), should be considered. Consequently, variables that primarily affect throughput rate such as permeability, inter-well distance, or injection/production pressures are addressed in the throughput calculation. Factors that affect volumetrics such as net pay, porosity, or pattern size will be normalized out of the results when the output is converted to dimensionless curves. It is important to use average values to represent porosity, water saturation, and net pay so that gravity effects are reasonably accounted for.

The dimensionless type curves generated by the reservoir simulations are then used to describe waterflood performance over the range of expected rock and fluid properties. These curves can be used in a spreadsheet that allows a user to input a set of parameters that describe the pattern and have the spreadsheet draw a dimensionless performance curve for the case in question. If the model builder is so inclined, the spreadsheet model can generate a dimensionless performance curve for <u>any</u> case within the range, by interpolating within the type curves. A spreadsheet model that incorporates a set of dimensionless curves and performs this interpolation is discussed in the next chapter.

CHAPTER 5

CASE STUDY – SOUTH SEA OILFIELD

The methodology described above is applied to an actual oilfield using real field data and information. Generic names are used because there is no reason to identify the field or formation. The field in question is a very large, waterflooded field of mid-to-late maturity. Despite its relative maturity, there are a number of opportunities and options to be evaluated. Consequently, there are many decisions regarding throughput acceleration options, infill drilling, and facility expansions yet to be made.

The geology and stratigraphy of this particular reservoir were studied and it was determined there were three major factors that affect waterflood performance: reservoir quality/continuity, permeability variation, and pattern geometry. It is important to understand why these variables are isolated for further analysis and how they vary across the field. A detailed description of the geology and stratigraphy is given below.

5.1 Geology of the South Sea Reservoir

The formation in question was deposited during Neocomian time and is divided into two members that are separated by a local, unconformity. The lower member consists of a heterolithic sequence of thinly interbedded sandstones, siltstones, and mudstones. The upper member is characterized by massive, bio-turbated sandstones and siltstones.

The trapping mechanism is a combination of stratigraphic pinchout and truncation against a local unconformity along the southern and western flanks of a south-east plunging antiform, and structural dip closure along the northern and eastern flanks. Faulting in the field is marked by two sets of faults. A set of northeast – southwest trending faults that were formed while the upper sand was being deposited. A second set of primarily north-south trending faults formed post-deposition. Compared to the many other fields around the world, this reservoir would be considered highly faulted.

The reservoir sandstones of the lower member (Z Sand) are thought to be detached or "beheaded" shallow marine deposits with a provenance to the northeast. Core evidence suggests

this sand was a storm dominated shelf deposit that was disconnected from the main source. These shoreface detached sand sheets show no evidence of shoreface, channel fill, or deltaic deposits in the immediate vicinity. The reasons for sand deposition at this location are attributed to the right combination of inherited topography, current energy, and water depth. Much of these deposits exhibit hummocky, cross-stratified character indicating deposition analogous to the current and wave effected inner shelf margin of the Atlantic shelf. This type of depositional environment leads to highly anisotropic properties which has significant impact on the producibility and floodability of the reservoir.

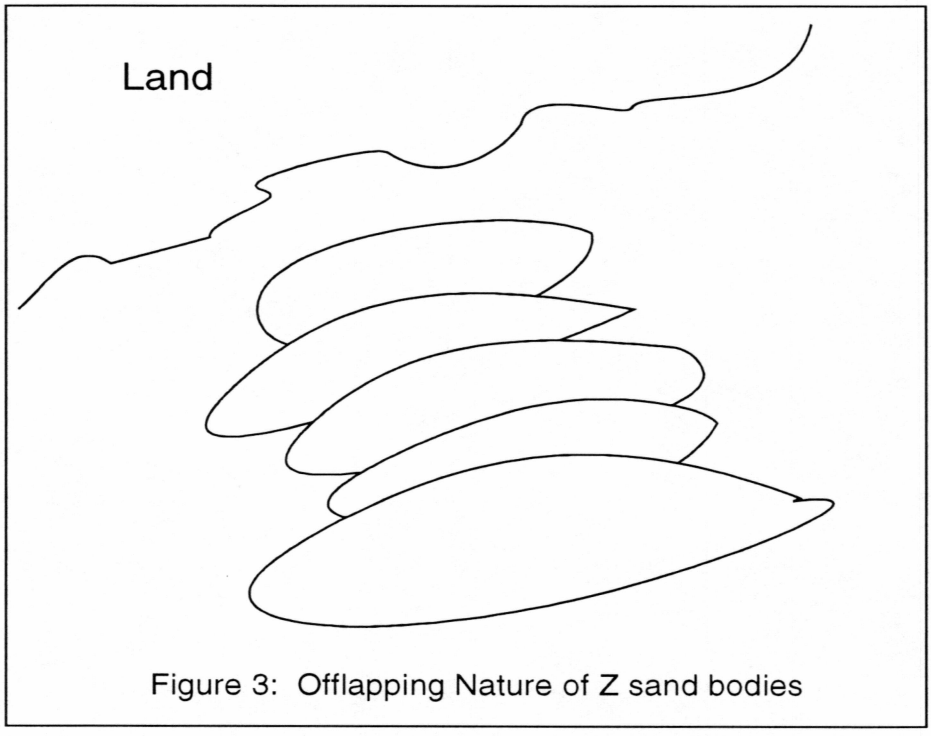

Figure 3: Offlapping Nature of Z sand bodies

This reservoir is divided into 5 sand bodies, Z1 through Z5, which exhibit an offlap pattern to the southeast with large, oblong shaped lenticular geometries with the strike axis in a northeast-southwest orientation. Figure 3 shows the offlapping nature of these sand bodies. Each of these individual units is composed of fine grained quartz arenite interbedded with siltstone and shales in regressive sequences up to 70 ft thick. The sandstones are fairly clean with less than 5% intergranular kaolinite and illite.

The frontal or beach side of the sand bodies exhibit thick sand packages of amalgamated cross-stratified hummocky deposits. This area of deposition experienced more wave and current action, which helped to sort and clean the sediment, but also scour any clay that was deposited between storm events. The distal or ocean side of the deposits had less energy, which resulted in considerably more mud deposits. These deposits show up as mudstone layers within the storm deposits, but also appear as thin, very fine clay or shale deposits between events. This part of the sand bodies has much less vertical permeability, and where the mudstones are draped over and encase the sands, have less lateral (horizontal) permeability as well.

The Z sand member has significant remaining reserves and therefore demands considerable attention and understanding to exploit this potential. The geologic model shows that continuity is a major concern in the Z sand member. Because of the relatively large well spacing at present, there is some percentage of net pay that is not continuous between wells. In order to predict the amount of pay that is continuous, and therefore the ultimate recovery with waterflood, it is necessary to define the location of each pattern in relation to the localized deposition of each Z sand sub-unit.

5.2 Lithofacies Interpretations of the Z Sand

The individual Z sand bodies (e.g. Z3, Z4) can exhibit pronounced lateral change in lithofacies due to the localized changes in wave and current energy during a storm. The slightest change in geometry or energy can alter the depositional process to cause considerable heterogeneity in a lateral sense. This imbricate nature of the storm generated sandstone beds is easy to see in cores as well as correlated cross-sections. Each sand has been categorized into 6 different lithofacies based on structure, shale geometries, and sand/shale ratios. These lithofacies are as follows:

Lithofacies H - Hummocky cross-stratified sandstone
Lithofacies F - Flaser bedded sandstone
Lithofacies W - Wavy bedded sandstone
Lithofacies L - Lenticular bedded sandstone
Lithofacies S - Mudstone with lenticular sandstone streaks
Lithofacies B - Bioturbated lenticular or wavy-bedded sandstone

These categories represent a continuum of sedimentation and are listed in order of decreasing wave and current energy. The type and thickness of each facies is also a function of the size and severity of the storm as well as the proximity to the shoreline and the corresponding water depth. Because lithofacies H and F make up 99% of the net pay, further discussion will be limited to these two.

Lithofacies H: Hummocky cross-stratified beds are sedimentary structures with medium to coarse grained "storm layers" interlayered or embedded in finer grain mudstones. The storm layers are medium to large scale concentrations of clean sands that are deposited during maximum sediment loading and during the higher energy intervals of the storm. The thin mudstone layers represent suspension type deposits of fine sediment during brief periods of low energy. The thin layers of mudstone follow a wavy pattern on a large scale but can appear as parallel layers at the core level. The layers can show vertical size grading as the energy of the storm subsides. These storm layers, also called tempestites, are best developed on the inner shelf, probably in water depths of 50'-120'. Although somewhat controversial, they are believed to form by a two stage process: 1.) Transport from the beach or source by storm generated turbulence, followed by 2.) reworking and selective sorting by asymmetrical oscillatory currents due to storm swells and waves propagating onshore.

Lithofacies F: Flaser bedded lamination is cross lamination in which mud streaks are preserved in the troughs of ripples, but incompletely or not at all on the crests. The structure is marked by wave ripple lamination with draping lamina sets, discordant internal truncation, and irregular boundaries. The smaller scale of this lithofacies, compared to the lithofacies H, and the increased concentration of mudstone suggests a lower energy area of deposition, i.e. deeper water. This lithofacies is often found below lithofacies H indicating a regressive sequence.

5.3 Depositional Character of the Z Sand (Lithofacies Sequences)

Each of the Z sand reservoir sub-units exhibit a shallowing upward trend based on grain size (coarsening upward), thickness trends (thickening upward), and vertical succession of lithofacies. Describing the character from a vertical perspective, the base of each unit is marked by current rippling. Above that, wave formed structures increase in concentration and scale. The upper section is dominated by hummocky cross-stratification, which in many cases is amalgamated into large sand packages. Finally, the entire unit is capped by a coarse lag or a bioturbated interval

and then in turn overlain by a thin, interstorm mudstone unit. This cyclic sequence is repeated within each sub-unit until deposition is interrupted by a major transgression, which is represented by a regionally extensive mudstone.

The estimated water depth at the point of maximum regression at each sub-unit cycle is approximately 50-100 feet. Water depths as deep as 350 ft are estimated in the distal parts of the cycle. Describing the character from a lateral perspective, the proximal or beach sides of the sandstone bodies consist of amalgamated packages of hummocky, cross-stratified facies and flaser bedded facies. In this area the lateral change and size sandstone lenses is dictated by the proximity to the shore face (source), and the slope of the shelf. The front of these bodies was in water depths that allowed wind and wave energy to scour inter-storm deposits, and deposit only the coarsest sediment available. The thick axial crest of the sand body consists of thick amalgamated packages where any remnants of suspension deposits between storms were removed. The distal side or ocean side of the sand body consists of much more mud deposits between events resulting in facies of wavy bedded sandstone shale (Lithofacies W) and shale with lenticular sandy streaks (Lithofacies L).

As an example of one interpretation of the lateral depositional character, the Z sand can be classified into 3 different sequences based on the relative location within the sand body as a whole. Sequence I, located on the beach side or updip terminus of the body is characterized by a thin upward coarsening sequence of facies. The bottom consists of an upward transition of lenticular and wavy-bedded lithofacies into flaser bedding and finally into a fairly thick (~4') package of cross-stratified hummocky sandstones.

Sequence II, located near the axial center of the sandstone body is downdip and makes up the thickest section of the unit. This area is characterized by a thick (~30-40') sequence of flaser bedded and hummocky cross-stratified beds followed by a single, thick amalgamated hummocky cross-stratified bed at the top. These amalgamated packages may be as thick as 15 feet, with evidence of multiple events, with little remnants of low-energy deposition.

Sequence III, located on the ocean or distal side near the downdip terminus of the body, is characterized by much more mud and shale with interbedded hummocky cross-stratified and lenticular wavy bedded structures. This area of the deposit had more accommodation space due to the deeper water depth and is thus the thickest of the three sequences. It is also here where

the wave and wind energy was dampened by deeper water to prevent the scouring of interstorm deposits. Also, due to its distal location, the sediment was much finer, consisting of more mud than Sequence I or II areas.

5.4 Reservoir Continuity, Effect on Floodability

Within the Z sand members, the thickness of individual beds depend on whether they are amalgamated or single event beds. Consequently, the thickness distributions are indicative of multiple events or single events. It is useful to understand these relationships as they have direct bearing on the prediction of reservoir continuity. In short, an amalgamated sequence of multiple events will have a higher probability of continuity between wells than a sequence of shale separated single events.

The distinguishing features of amalgamated beds are sand-on-sand scoured contacts or contacts defined by individual mudstone drapes within a package bounded by continuous shale barriers. The distinguishing features of individual beds or events are thin lenticular and wavy bedded lithofacies separated by shale barriers. These beds are vertically isolated from beds above and below by continuous, unscoured shale barriers. Most single event sandstone beds are less than 6 inches thick.

Regressive lower shoreface, inner shelf sandstones such as those of the Z sand are characterized by their numerous vertical permeability barriers in the form of continuous shales and discontinuous mudstones. These layers of reservoir quality sandstone are imbricate or shingle like in nature in a southeasterly downdip direction, similar to the imbrication of the major members themselves. This imbrication has significant impact on the horizontal permeability on a macroscopic level. Consequently, the floodability across distances of 160 acre well spacing (~2600') is highly dependent on the volume of continuous sandstone from well to well, which can be significantly less than the calculated net pay in a particular pair of wells.

It is important to note that significant permeability heterogeneities exist not only between layers but also within layers. These barriers within the sandstones can not be traced from well to well, so in order to account for their affects on the waterflood performance, an accurate geologic model must be assembled.

As one would imagine, based on the lithofacies descriptions and depositional character, reservoir properties (porosity, permeability) are largely dependent upon lithofacies in the Z interval. Whereas porosity is a function of sand-silt-clay ratio, permeability is controlled by bedding structure. Vertical permeability is largely dependent on the number and thickness of the individual mudstone laminae. Horizontal permeability on the other hand is highly dependent on the localized extent of the amalgamated sands, and the extent of mud drapes that tend to encase the individual sand bodies. This prediction of horizontal permeability as a function of the geologic model is critical to predicting oil recoveries with a waterflood process.

5.5 Structural Faulting, Effect on Pattern Shape

In addition to the stratigraphic complexities just described, this reservoir would be considered highly faulted. Much the way stratigraphic heterogeneities affect reservoir continuity, faulting also has a significant effect on waterflood performance. Because faults interrupt the "natural flow" from an injector to a producer, they tend to lower recovery for a given volume of water injected. In some cases, the inefficiencies caused by faults are not significant. In other cases, where a large part of a pattern is isolated from the short streamlines, the recovery in the pattern can suffer significantly. Because it is more difficult to classify the effects of faulting, the estimation of recovery as a function of faulting is a bit more subjective. One such classification system is introduced in the following section.

5.6 Reservoir Descriptions used in Simulations

Given the stratigraphy and faulting just described, there are a number of types of reservoir models that could be built to better understand potential depletion strategies. As discussed earlier, the traditional approach would be to build a very detailed reservoir model for a specific area that captures all important heterogeneities. Such a model could be used to test various depletion mechanisms such as miscible flooding, or could be used to help identify unswept areas where a new well might be located.

A second approach would be to characterize the geology with a set of simplistic descriptions that capture the attributes that most affect waterflood performance. To serve as the basis of an integrated model, this is the approach that has been applied in this study. The lithofacies and stratigraphy of the Z sand is resolved into a set of descriptions that capture the variation in

permeability and its effects on continuity. The effects of various faulting geometries is captured with "pseudo pattern shapes" to estimate the inefficiencies caused by faulting.

The reservoir models used for this work are based on the understanding of the stratigraphy and structural setting of the Z sand. In short, permeability variation and continuity is a function of the lithofacies which is a function of where and how the sands were deposited. Pseudo pattern shapes, or skew factor, are used to account for the faulting effects. This approach is designed to isolate the value of increased throughput and/or the effects of tighter spaced wells. It is believed that this approach is valid for drawing general conclusions about the benefits of various re-development options. However, it is suggested that site specific knowledge of the stratigraphy and faulting of a potential area are used in subsequent evaluations of an area.

Because the reservoir simulation will be used to predict waterflood performance, and not throughput rate, and because these curves will be normalized on a hydrocarbon pore volume basis, there are a number of variables that can be eliminated from the sensitivity analysis. The first set of variables that can be eliminated are those used in the hydrocarbon pore volume calculation, namely, porosity, water saturation, and net pay. By scaling the simulation results by hydrocarbon pore volume, the effect of porosity, water saturation and net pay on volume is accounted for. It is important to note that the porosity and water saturation of the Z sand does not vary that much. For all wells with a net pay in the Z sand, the 80% confidence interval of net pay ranges from 17% to 23%. Similarly, the 80% range on porosity is 19% to 25%.

Other sensitivities can be eliminated because those variables that affect throughput rate, such as permeability and net pay, will be accounted for in the throughput rate calculation. The utilization of the Darcy flow equation to estimate throughput rate will account for the range of variables like permeability, skin, net pay, and pressure drop. Consequently, only those geological factors that affect waterflood recovery (as defined by WOR vs. percent recovery or percent recovery vs. HCPWVI) need be isolated. As a result, the number of reservoir descriptions (i.e. 45 in this case) is reasonable. These 45 reservoir descriptions result from a combination of three levels of "reservoir quality/continuity", three levels of permeability variation, and five types of pattern shapes or levels of "skewness". Each of these descriptions is described below.

5.6.1 Reservoir Quality/Continuity

The range on reservoir continuity is divided into three categories that are simply referred to as good, fair, and poor. A description of the properties, and their relationship to the stratigraphy is given below.

Good – Good continuity is meant to describe those areas of the Z sand that show good sand continuity based on its lithofacies. A good sand package would be one with a very large concentration of amalgamated hummocky cross stratified (HCS) beds with very little mudstone deposits within the beds. This type of sand would be found near the top of sequence I and sequence II type deposits. This description has a reservoir continuity of 95% on 160 acre spacing and 99% at 80 acre spacing. The kv/kh ratio is 0.01.

Note: Percent continuity is defined as that percent of net pay that is continuous between the injector and producer. Net pay is that pay that is above the porosity and water saturation cutoff as defined in the log model. If the net pay is 90% and the net pay is 30 feet, then a layer or layers summing to 3 feet thick will have a permeability barrier between the injector and producer and will not be floodable. This layer(s) will be completely encased in shale to prevent flow around the barrier.

Fair – Fair continuity is meant to describe those areas of the Z sand that have fair continuity based on its lithofacies. A fair sand package would have some amalgamated HCS beds, more non-amalgamated beds, and some flaser beds. This type of sand would be found near the base of sequence I and sequence II type deposits, as well as near the top of sequence III deposits. This description has a reservoir continuity of 90% on 160 acre spacing and 97% at 80 acre spacing. The kv/kh ratio is 0.001.

Poor – Poor continuity is meant to describe those areas of the Z sand that have poor continuity based on its lithofacies. A poor sand package would be one with very little amalgamated HCS beds. Instead, the sand would have a considerable amount of mudstone deposits between HCS beds and within flaser beds. This type of sand would be found primarily in sequence III deposits. This description has a reservoir continuity of 80% on 160 acre spacing and 95% at 80 acre spacing. The kv/kh ratio is 0.0001.

5.6.2 Permeability Variation; Dykstra-Parsons[10] Coefficient

Within each level of reservoir quality/continuity are three levels of permeability variation as described with a Dykstra-Parsons[10] coefficient. The definition of the Dykstra-Parsons coefficient is given by equation 1:

$$V = (\log k_{avg} - \log k_{\sigma})/\log k_{avg} \qquad (1)$$

where: k_{avg} = mean permeability

k_{σ} = permeability at one standard deviation from mean

In this equation, the Permeability Variation (Dykstra-Parsons coefficient), V, is defined as the difference between the mean permeability, and the permeability of one standard deviation from the mean, divided by the mean of permeability, when all values are converted to log scale. The basis for this representation of variation is that permeability can be described as a log-normally distributed parameter. A coefficient of 1.0 would have no variation. Large variation would be described with a number closer to 0. In the context of real oilfields, a coefficient of 0.5 would describe zones with high variation (poor conformance), and a coefficient of 0.9 would describe zones with low variation (good conformance).

For the case of the Z sand descriptions, a distinct description has been created for each classification of reservoir quality/continuity to represent the range in permeability variation. These three cases of permeability variation are described with Dykstra-Parsons coefficients of 0.9 for little variation, 0.7 for moderate variation, and 0.5 for much variation.

The 9 combinations of reservoir quality/continuity and Dykstra-Parsons coefficients are shown in the following tables. Tables 1, 2, and 3 represent the three levels of reservoir quality/continuity: good, fair, poor, respectively. The three tables on each page represent the three levels of permeability variation with coefficients of 0.9, 0.7, and 0.5. The result is nine different reservoir descriptions designed to represent the continuum of variation of the two most important rock properties that affect waterflood performance.

Table 1: Simulator Input
Good Reservoir Quality/Continuity

Net Pay = 45'; Average Perm = 120 md; Continuity = 96%; kv:kh = .01

Zone	Thickness	Porosity	h*Por	Perm	Log Perm	kh	log kh	Discontinuous?
1	3	0.17	0.51	70	1.85	210	2.322	
2	4	0.23	0.92	120	2.08	480	2.681	
3	6	0.25	1.5	170	2.23	1020	3.009	
4	3	0.19	0.57	70	1.85	210	2.322	
5	5	0.21	1.05	150	2.18	750	2.875	
6	4	0.22	0.88	130	2.11	520	2.716	
7	2	0.19	0.38	60	1.78	120	2.079	Y
8	3	0.21	0.63	110	2.04	330	2.519	
9	5	0.26	1.3	160	2.20	800	2.903	
10	4	0.21	0.84	110	2.04	440	2.643	
11	2	0.20	0.4	40	1.60	80	1.903	
12	4	0.23	0.92	110	2.04	440	2.643	

	Wtd Avg	Sum h*Por				
Net Pay	Porosity	9.9	Wtd Avg k		Total kh		% Continuous
45	0.22		120		5400		95.5%
Dykstra-Parsons Permeability Variation				0.90		0.868	

Zone	Thickness	Porosity	h*Por	Perm	Log Perm	kh	log kh	Discontinuous?
1	3	0.17	0.51	10	1.00	30	1.477	
2	4	0.23	0.92	120	2.08	480	2.681	
3	6	0.25	1.5	170	2.23	1020	3.009	
4	3	0.19	0.57	30	1.48	90	1.954	
5	5	0.21	1.05	120	2.08	600	2.778	
6	4	0.22	0.88	15	1.18	60	1.778	
7	2	0.19	0.38	65	1.81	130	2.114	Y
8	3	0.21	0.63	220	2.34	660	2.820	
9	5	0.26	1.3	270	2.43	1350	3.130	
10	4	0.21	0.84	200	2.30	800	2.903	
11	2	0.20	0.4	10	1.00	20	1.301	
12	4	0.23	0.92	40	1.60	160	2.204	

	Wtd Avg	Sum h*Por				
Net Pay	Porosity	9.9	Wtd Avg k		Total kh		% Continuous
45	0.22		120		5400		95.5%
Dykstra-Parsons Permeability Variation				0.70		0.734	

Zone	Thickness	Porosity	h*Por	Perm	Log Perm	kh	log kh	Discontinuous?
1	3	0.17	0.51	10	1.00	30	1.477	
2	4	0.23	0.92	18	1.26	72	1.857	
3	6	0.25	1.5	110	2.04	660	2.820	
4	3	0.19	0.57	9	0.95	27	1.431	
5	5	0.21	1.05	165	2.22	825	2.916	
6	4	0.22	0.88	15	1.18	60	1.778	
7	2	0.19	0.38	6	0.78	12	1.079	Y
8	3	0.21	0.63	220	2.34	660	2.820	
9	5	0.26	1.3	270	2.43	1350	3.130	
10	4	0.21	0.84	410	2.61	1640	3.215	
11	2	0.20	0.4	2	0.30	4	0.602	
12	4	0.23	0.92	15	1.18	60	1.778	

	Wtd Avg	Sum h*Por				
Net Pay	Porosity	9.9	Wtd Avg k		Total kh		% Continuous
45	0.22		120		5400		95.5%
Dykstra-Parsons Permeability Variation				0.50		0.579	

Table 2: Simulator Input
Fair Reservoir Quality/Continuity

Net Pay = 35'; Average Perm = 80 md; Continuity = 90%; kv:kh = .001

Zone	**Thickness**	**Porosity**	h*Por	**Perm**	Log Perm	kh	log kh	**Discontinuous?**
1	**2**	**0.17**	0.34	**50**	1.70	100	2.000	
2	**3**	**0.23**	0.69	**90**	1.95	270	2.431	
3	**4**	**0.25**	1	**115**	2.06	460	2.663	
4	**2**	**0.19**	0.38	**30**	1.48	60	1.778	
5	**3**	**0.21**	0.63	**60**	1.78	180	2.255	
6	**5**	**0.26**	1.3	**110**	2.04	550	2.740	
7	**1.5**	**0.20**	0.3	**50**	1.70	75	1.875	**Y**
8	**2**	**0.21**	0.42	**60**	1.78	120	2.079	**Y**
9	**2.5**	**0.24**	0.6	**90**	1.95	225	2.352	
10	**4**	**0.23**	0.92	**100**	2.00	400	2.602	
11	**2**	**0.20**	0.4	**40**	1.60	80	1.903	
12	**4**	**0.18**	0.72	**70**	1.85	280	2.447	

	Wtd Avg	Sum h*Por				
Net Pay	Porosity	7.7	Wtd Avg k		Total kh	% Continuity
35	0.22		**80**		2800	90.0%

Dykstra-Parsons Permeability Variation **0.90**

Zone	**Thickness**	**Porosity**	h*Por	**Perm**	Log Perm	kh	log kh	**Discontinuous?**
1	**2**	**0.17**	0.34	**30**	1.48	60	1.778	
2	**3**	**0.23**	0.69	**160**	2.20	480	2.681	
3	**4**	**0.25**	1	**60**	1.78	240	2.380	
4	**2**	**0.19**	0.38	**15**	1.18	30	1.477	
5	**3**	**0.21**	0.63	**190**	2.28	570	2.756	
6	**5**	**0.26**	1.3	**75**	1.88	375	2.574	
7	**1.5**	**0.20**	0.3	**20**	1.30	30	1.477	**Y**
8	**2**	**0.21**	0.42	**15**	1.18	30	1.477	**Y**
9	**2.5**	**0.24**	0.6	**30**	1.48	75	1.875	
10	**4**	**0.23**	0.92	**180**	2.26	720	2.857	
11	**2**	**0.20**	0.4	**5**	0.70	10	1.000	
12	**4**	**0.18**	0.72	**45**	1.65	180	2.255	

	Wtd Avg	Sum h*Por				
Net Pay	Porosity	7.7	Wtd Avg k		Total kh	% Continuity
35	0.22		80		2800	90.0%

Dykstra-Parsons Permeability Variation **0.70**

Zone	**Thickness**	**Porosity**	h*Por	**Perm**	Log Perm	kh	log kh	**Discontinuous?**
1	**2**	**0.17**	0.34	**20**	1.30	40	1.602	
2	**3**	**0.23**	0.69	**165**	2.22	495	2.695	
3	**4**	**0.25**	1	**4**	0.60	16	1.204	
4	**2**	**0.19**	0.38	**5**	0.70	10	1.000	
5	**3**	**0.21**	0.63	**310**	2.49	930	2.968	
6	**5**	**0.26**	1.3	**75**	1.88	375	2.574	
7	**1.5**	**0.20**	0.3	**15**	1.18	22.5	1.352	**Y**
8	**2**	**0.21**	0.42	**6**	0.78	12	1.079	**Y**
9	**2.5**	**0.24**	0.6	**15**	1.18	37.5	1.574	
10	**4**	**0.23**	0.92	**180**	2.26	720	2.857	
11	**2**	**0.20**	0.4	**3**	0.48	6	0.778	
12	**4**	**0.18**	0.72	**34**	1.53	136	2.134	

	Wtd Avg	Sum h*Por				
Net Pay	Porosity	7.7	Wtd Avg k		Total kh	% Continuity
35	0.22		80		2800	90.0%

Dykstra-Parsons Permeability Variation **0.50** 0.566

Table 3: Simulator Input
Poor Reservoir Quality/Continuity

Net Pay = 25'; Average Perm = 40md; Continuity = 80%; kv:kh = .0001

Zone	Thickness	Porosity	h*Por	Perm	Log Perm	kh	log kh	Discontinuous?
1	**1**	**0.17**	0.17	**30**	1.48	30	1.477	
2	**2**	**0.21**	0.42	**45**	1.65	90	1.954	
3	**3**	**0.23**	0.69	**50**	1.70	150	2.176	
4	**1**	**0.19**	0.19	**20**	1.30	20	1.301	**Y**
5	**2**	**0.21**	0.42	**30**	1.48	60	1.778	
6	**3**	**0.26**	0.78	**55**	1.74	165	2.217	
7	**1**	**0.20**	0.2	**20**	1.30	20	1.301	**Y**
8	**2**	**0.21**	0.42	**35**	1.54	70	1.845	**Y**
9	**4**	**0.24**	0.96	**40**	1.60	160	2.204	
10	**1**	**0.18**	0.18	**25**	1.40	25	1.398	**Y**
11	**2**	**0.19**	0.38	**45**	1.65	90	1.954	
12	**3**	**0.23**	0.69	**40**	1.60	120	2.079	

Net Pay	Wtd Avg Porosity	Sum h*Por	Wtd Avg k		Total kh		% Continuous
25	0.22	5.5	**40**		1000		80.0%
Dykstra-Parsons Permeability Variation				**0.90**		0.805	

Zone	Thickness	Porosity	h*Por	Perm	Log Perm	kh	log kh	Discontinuous?
1	**1**	**0.17**	0.17	**5**	0.70	5	0.699	
2	**2**	**0.21**	0.42	**10**	1.00	20	1.301	
3	**3**	**0.23**	0.69	**45**	1.65	135	2.130	
4	**1**	**0.19**	0.19	**15**	1.18	15	1.176	**Y**
5	**2**	**0.21**	0.42	**20**	1.30	40	1.602	
6	**3**	**0.26**	0.78	**70**	1.85	210	2.322	
7	**1**	**0.20**	0.2	**5**	0.70	5	0.699	**Y**
8	**2**	**0.21**	0.42	**35**	1.54	70	1.845	**Y**
9	**4**	**0.24**	0.96	**40**	1.60	160	2.204	
10	**1**	**0.18**	0.18	**15**	1.18	15	1.176	**Y**
11	**2**	**0.19**	0.38	**35**	1.54	70	1.845	
12	**3**	**0.23**	0.69	**85**	1.93	255	2.407	

Net Pay	Wtd Avg Porosity	Sum h*Por	Wtd Avg k		Total kh		% Continuous
25	0.22	5.5	40		1000		80.0%
Dykstra-Parsons Permeability Variation				**0.70**		0.627	

Zone	Thickness	Porosity	h*Por	Perm	Log Perm	kh	log kh	Discontinuous?
1	**1**	**0.17**	0.17	**2**	0.30	2	0.301	
2	**2**	**0.21**	0.42	**15**	1.18	30	1.477	
3	**3**	**0.23**	0.69	**40**	1.60	120	2.079	
4	**1**	**0.19**	0.19	**19**	1.28	19	1.279	**Y**
5	**2**	**0.21**	0.42	**160**	2.20	320	2.505	
6	**3**	**0.26**	0.78	**100**	2.00	300	2.477	
7	**1**	**0.20**	0.2	**5**	0.70	5	0.699	**Y**
8	**2**	**0.21**	0.42	**10**	1.00	20	1.301	**Y**
9	**4**	**0.24**	0.96	**20**	1.30	80	1.903	
10	**1**	**0.18**	0.18	**10**	1.00	10	1.000	**Y**
11	**2**	**0.19**	0.38	**2**	0.30	4	0.602	
12	**3**	**0.23**	0.69	**30**	1.48	90	1.954	

Net Pay	Wtd Avg Porosity	Sum h*Por	Wtd Avg k		Total kh		% Continuous
25	0.22	5.5	40		1000		80.0%
Dykstra-Parsons Permeability Variation				**0.50**		0.501	

5.6.3 Pattern Shapes, Skew Factor

The classification system used to quantify the effects of faulting is designed to estimate the volume of a pattern that is subject to "inefficient flooding". The definition of skew factor is given by equation 2.

$$\text{Skew Factor} = (A + B)/A \qquad (2)$$

where: A = well flooded region
B = poorly flooded region

This estimate of the size of the poorly flooded area is described with the term "skew factor", where 1.0 is balanced and symmetrical, and a skew factor of 1.5 would have an area equivalent to 50% of the well flooded area that is inefficiently flooded. To better describe this classification methodology, a number of examples are presented.

Example 1: Skew Factor = 1.33

A skew factor of 1.33 means that an area equivalent to 33% of the well flooded area is being poorly flooded. Patterns that might look like this are shown below. [Note that in these cases the poorly flooded area (denoted with a B, B1, or B2) is about 33% of the area of the well flooded region.]

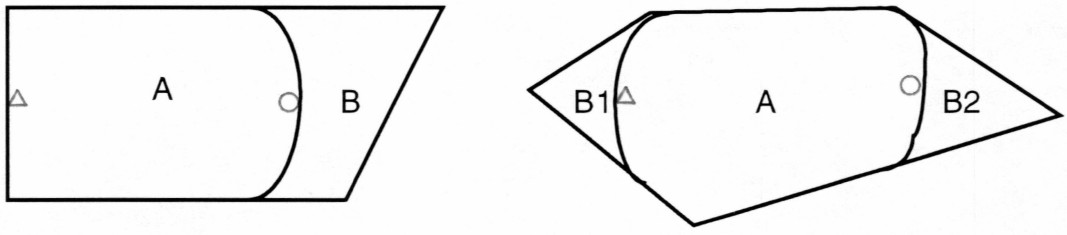

Figure 4: Patterns with skew factor of 1.33

Example2: Skew Factor = 1.67

A skew factor of 1.67 means that an area equivalent to 67% of the well flooded area is being poorly flooded. Patterns meeting this criteria might look like the following:

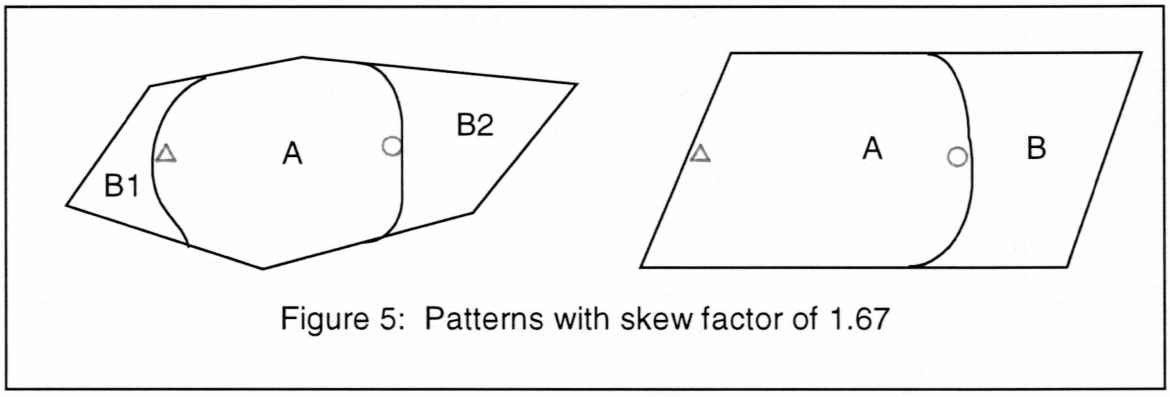

Figure 5: Patterns with skew factor of 1.67

It was also found that it is important to designate whether the skewed area is close to the injector or close to the producer. It appears that an under flooded area near an injector has less recovery than an equivalent area near a producer. This may be explained by the fact that an unflooded area near a producer will still produce some oil as primary production. Another reason is that streamlines are more likely to push oil into a dead corner if the area is near an injector. Because of this effect, five "skew factors" have been designated to describe the range of pattern shapes as follows:

1. Skew Factor 1.0 – 0% inefficiently flooded area
2. Skew Factor 1.33I – 33% inefficiently flooded area, skewed near injector
3. Skew Factor 1.33P – 33% inefficiently flooded area, skewed near producer
4. Skew Factor 1.67I – 67% inefficiently flooded area, skewed near injector
5. Skew Factor 1.67P – 67% inefficiently flooded area, skewed near producer

5.7 Simulation Datasets

Given the combination of three levels of reservoir quality/continuity, three levels of permeability variation, and five pattern geometries, there are a total of 45 different datasets for reservoir simulation. The simulations were performed with a proprietary, keyword driven, black oil simulator

that was available to the author. A sample input dataset is shown in Appendix A. The PVT properties and relative permeability tables were based on average properties for the reservoir in question.

The input dataset is divided into nine sections as follows:

1. Grid Definition
2. Fluid Properties
3. Saturation Functions
4. Reservoir Description
5. Edge Cell Modifiers
6. Miscellaneous Initial Data
7. Recurrent Data
8. Well Data
9. Time Step Controls

The assumptions and data of each section are described in the following sections.

5.7.1 Grid Definition

The choice of grid size and grid definition is usually a trade-off between model accuracy and computational time. For the 45 datasets used in this study, a three dimensional model was chosen with half-acre grid blocks and 12 flow units. It was found that predictive runs took about 60 to 90 minutes, on an IBM RS6000 RISC computer, to predict rate and recovery for a 50 year time horizon. This seemed like an appropriate trade-off of grid resolution and computing time for this study.

The grid dimensions for the symmetrical pattern case (skew factor 1.0) were 18 blocks in the east-west direction, 9 blocks in the north-south direction, and 12 layers, for a total of 1944 cell blocks. Each block was 147 feet in the x-y direction to yield blocks of approximately one-half acre. The dimensions in the z direction ranged from .5 feet to 6 feet as shown in Tables 1, 2, and 3.

The grid dimensions for the skewed patterns were 24 X 9 and 30 X 9 for a skew factor of 1.33 and 1.67 respectively. The sample dataset in Appendix A is a producer skewed pattern of skew 1.33.

This geometry has 6 blocks on the opposite (from injector) side of the producer for a dimension of 24 X 9 for a total of 216 grids in the x-y direction as shown below.

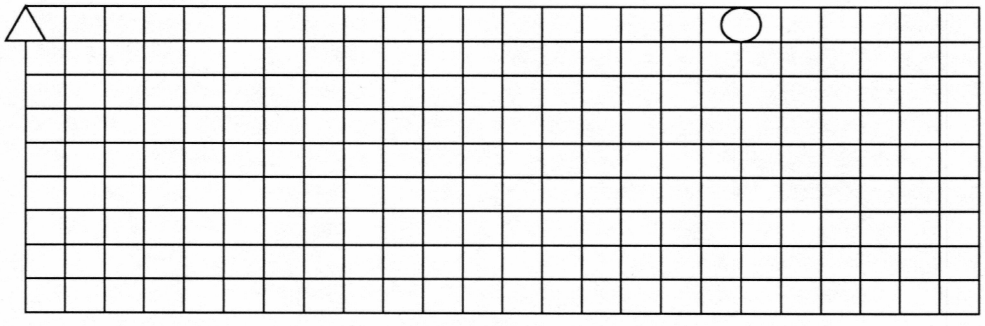

Figure 6: Grid Cell Geometry for sample dataset with skew factor of 1.33p

5.7.2 Fluid Properties

The fluid property section is designed to describe the static fluid properties as well as those properties that are a function of the pressure and temperature of the fluid. This section describes the system as a water-oil-gas system and gives the API gravity of the crude and static properties of water. It also gives the temperature of the reservoir.

The pressure-volume-temperature (PVT) table gives the standard set of reservoir properties as a function of pressure. This includes (in the order shown): Pressure, Oil Formation Volume Factor (BOT), Gas Formation Volume Factor (BGT), Gas-Oil Ratio (RST), Viscosity of Oil (VOT), and Viscosity of Gas (VGT).

For this study the PVT properties were assumed to be constant for all datasets. If one is working a field where a property such as API gravity varies across the field, the user may need to define several PVT regions for each region to account for the range in API gravity.

5.7.3 Saturation Functions

The saturation functions (a.k.a. relative permeability curves) are given for three sets of initial water saturation states. In this case, the three states are Swi = 0.15, 0.5, and 1.0. The first set of curves is meant to describe the primary imbibition case, while the third set is meant to describe the primary drainage case. The intermediate value case (Swi = 0.5) allows for the user to specify different relative permeability curve shapes depending on the initial water saturation of the grid block. In other words, it is an easy way to allow for multiple saturation functions for different initial saturation states.

5.7.4 Reservoir Description

The reservoir description section gives the absolute permeability for each grid block. In the sample dataset the permeability in the z direction corresponds to the "fair" reservoir description with a Dykstra-Parsons coefficient of 0.7 as shown in Table 2. The barriers are meant to describe those layers that are discontinuous between wells. In this dataset, layers 7 and 8 are discontinuous about halfway between the two wells.

5.7.5 Edge Cell Modifiers

Edge cell modifiers are necessary because the simulations are based on the smallest element of symmetry with pattern boundaries designed to be no-flow boundaries. For the numerical simulation to properly mimic an actual pattern, the properties of the edge cells must be modified. These pore volume and transmissibility modifiers are necessary to create soft boundaries, rather than hard boundaries. In this section, the pore volume and transmissibility in the z direction of all edge cells is multiplied by 0.5. Also, the transmissibility in the X direction is multiplied by 0.5 for the north and south boundaries, and the transmissibility in the y direction is multiplied by 0.5 for the east and west boundaries.

5.7.6 Miscellaneous Initial Data

The miscellaneous initial data section provides such information as rock compressibility, depth of the top layer, initial water saturation, and the initial reservoir pressure.

5.7.7 Recurrent Data

Recurrent data is that data that the reservoir simulator needs to perform the mathematical calculations. This includes information about which solver to use and the time step sequences. The fully implicit technique (also known as the Backward-Euler technique) was employed here. No effort was paid to which technique (implicit versus IMPES) was most suitable. Given that the datasets were fairly small, and the runs were expected to be stable, the implicit technique was considered suitable.

The solver used in this simulation is the sparse linear algebra package with stabilized bi-conjugate gradient technique. The hydrocarbon pore volume calculation used to normalize the output to various size patterns based the calculation on the average calculated pattern pressure. However, this was found to introduce a slight error when comparing patterns. It is recommended that the HCPVI calculation be based on a standard pressure (e.g. 3000 psi) so that the normalization is based on a standardized, static volume irrespective of pattern pressure.

5.7.8 Well Data

The well data section gives the relative location of the wells and how the wells are to be injected and produced. In this simulation, well 1 is the injector and is located in cell 7,1 and perforated in all layers. Well 2 is the producer and is located in cell 24,1 and also perforated in all layers. The completion must be modified to account for the quarter symmetry pattern.

Both injector and producer are placed on "pressure control" with properties typical of the field in question. The pressure control method is best for replicating steady state conditions for a pattern. The bottom hole injection pressure of 4000 psi and bottom hole flowing pressure of 1500 psi is typical for injectors and producers of this field. An 8-1/2" production hole that is fracture stimulated to a skin of –3 is also typical of wells in this field.

5.7.9 Time Step Controls

The time step controls instruct the program to print information at specific time intervals, in this case every quarter (91.25 days). Information that is output to a file include well data (production, injection data) and material balance data. The program is instructed to run for 100 years (36,500 days).

5.8 Simulation Results, Observations

The results of the 45 simulations are shown in Figures 9-20 in the Appendix B. A subset of these graphs is discussed in this section.

- Figures 9, 10, and 11 show the total variation in recovery efficiency for the range of skew factor and permeability variance for each classification of reservoir quality. The total range of recovery at a WOR of 30 for all variables is 24% to 46%. Prior to this work, many surveillance and reservoir engineers believed the recovery of each pattern was much closer to an average figure of 38%. These graphs show that the range of reservoir performance is much greater than previously thought.
- Figures 15 and 16 show that reservoir quality/continuity has less impact than expected. For example, the recovery between the 90% continuity case (fair quality), and the 80% continuity case (poor quality) is much less than the average recovery (~40%) times the difference in floodable pay (10%). This can be explained by the fact that those layers that are not continuous, have lower permeability, lower porosity, and much lower recovery. In other words, the recovery of a description with 10% less continuous pay is not 10% lower because the pay that is not continuous has less pore volume and a slower flood rate.
- Figures 17 and 18 show that the recovery difference across the range of Dykstra-Parsons coefficient is significant. This highlights the fact that when defining recovery at a specific WOR cutoff (i.e. 30), the layers that are very tight and flood very slowly will recover very little of their oil, relative to the faster flooded layers. On the other hand, if the permeability contrast is small, all layers will flood at about the same pace and water breakthrough will be delayed. This is highlighted by Figure 16, which shows the range in water breakthrough of 7% of recovery at a Dykstra-Parsons coefficient of 0.5, to 20% of recovery at a coefficient of 0.9.
- Figures 19 and 20 show how the pattern shape and skew factor has a significant impact on recovery. This highlights the inefficiencies caused by significant faulting. This might lead to conclusions about the value of infill drilling to re-define pattern shapes.
- Figures 18 and 20 highlight the value of information of knowing the breakthrough timing. Both of these plots show that once breakthrough has occurred, the variation on ultimate recovery for the range of type curves is very small. This would indicate that a straight line trend of the log WOR vs. cumulative production curve (i.e. above a WOR = 1) is not necessary to accurately predict watercut behavior and ultimate recovery. Once water breakthrough has

occurred (i.e. WOR = 0.05 or 0.1), any type curve can be applied to reasonably predict future performance.

For the particular field that these simulations were based on, the observations are quite valuable. However, from a methodology standpoint, the point of these simulations was not to confirm the obvious – i.e. poor waterflood performance can be expected when permeability variation is high and/or pattern shapes are asymmetrical. These simulations were done to quantify the differences so that cash flow differences can eventually be calculated. This leads to the design of the optimal depletion scheme that considers the effects of heterogeneities.

5.9 Spreadsheet Based Recovery Prediction Tool

The simulation results in raw form, as shown in the earlier graphs, may help quantify the competing effects of reservoir quality, permeability variation, and pattern shape for distinct cases, but are difficult to apply to real world examples. To make the results easier to apply, a spreadsheet program was built that allows the user to enter any level of permeability variation or skew factor for a given reservoir quality descriptor, and have a custom curve calculated. There are a number of ways that this "interpolation" could have been achieved, including genetic algorithms or four dimensional curve fits. For this exercise, a series of linear interpolations are employed to arrive at the custom curve.

The program is presented as a user-friendly spreadsheet as shown in Figure 7. The user is asked for the reservoir quality (Good, Fair, Poor), the Dykstra-Parsons coefficient (any real number from 0.9 to 0.5), a skew factor from 1.0 to 1.67, and the percent of skewed area nearest the producer. Once the user has entered this information, the waterflood performance curve matching these conditions is drawn on the screen. The performance is characterized with two curves. The first is Log WOR versus percent recovery. The second is percent recovery versus HCPVWI. The spreadsheet is also set up for the user to input a second set of conditions so that an onscreen comparison can be made of the recovery efficiency and water cut behavior.

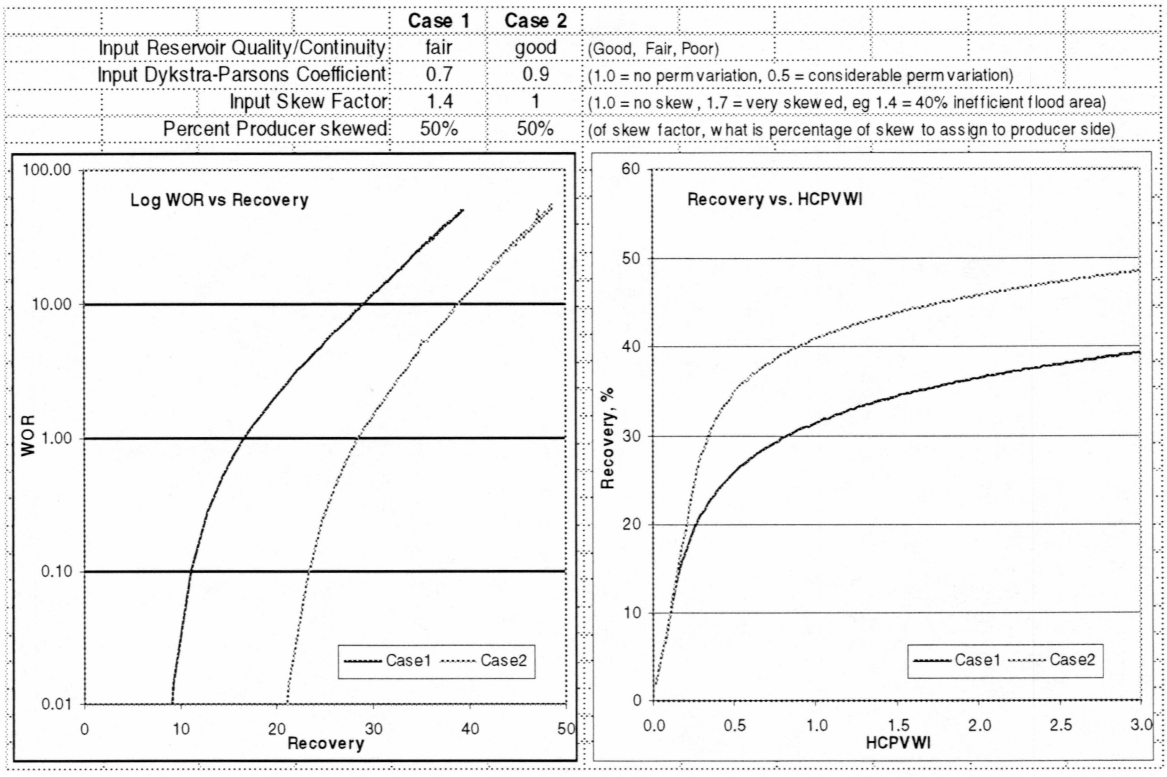

Figure 7: I/O Screen of Spreadsheet Based Recovery Prediction Tool

CHAPTER 6

USES OF DIMENSIONLESS RECOVERY CURVES

The simulation based dimensionless performance curves can be used in a number of different applications. To demonstrate the utility of the proposed methodology, three applications of the technique are discussed. These are: (1.) comparing actual production data to predicted performance, (2.) full-field forecasts by summing well performance predictions, and (3.) as the foundation of an integrated reservoir and economic evaluation tool.

6.1 Comparison of Actual Production to Predicted Performance

One of the advantages of dimensionless performance curves is that they can be formatted in such a way to make it easy to compare with actual field data. For example, the log WOR versus percent recovery curve can be easily compared to a standard "cut-cum" curve once the cumulative oil production has been normalized to percent recovery. Although the idea of normalizing production on a percent recovery basis is not new, the normalized "cut-cum" technique appears to be a variation that was not found elsewhere in the literature.

The normalized "cut-cum" technique allows the user to gain insights about what factors affect breakthrough timing and the slope of the curve. This technique requires that some estimate be made of the size of the floodable area. Once this estimate is made, the logarithm of the water-oil-ratio is plotted versus percent recovery. The range in breakthrough timing and normalized slopes should relate to the rock and fluid properties unique to that pattern.

Figure 8 shows a plot of actual production data that has been normalized to percent recovery. Also shown is the simulation-based dimensionless recovery curve that best matches the production data. It should be noted that this well was drilled into an area that had prior water injection and therefore had a small amount of water production from start-up. This explains the constant but very low WOR (~.05) until true water breakthrough occurred.

In this pattern, based on reviews of nearby cores and discussions with the geologist, the surveillance engineer thought the reservoir quality was good, and the permeability variation was low. He also had some expectation that part of the pattern was being poorly flooded. He was unsure however whether this area of poorly flooded pattern was 10% or 30% of the well flooded

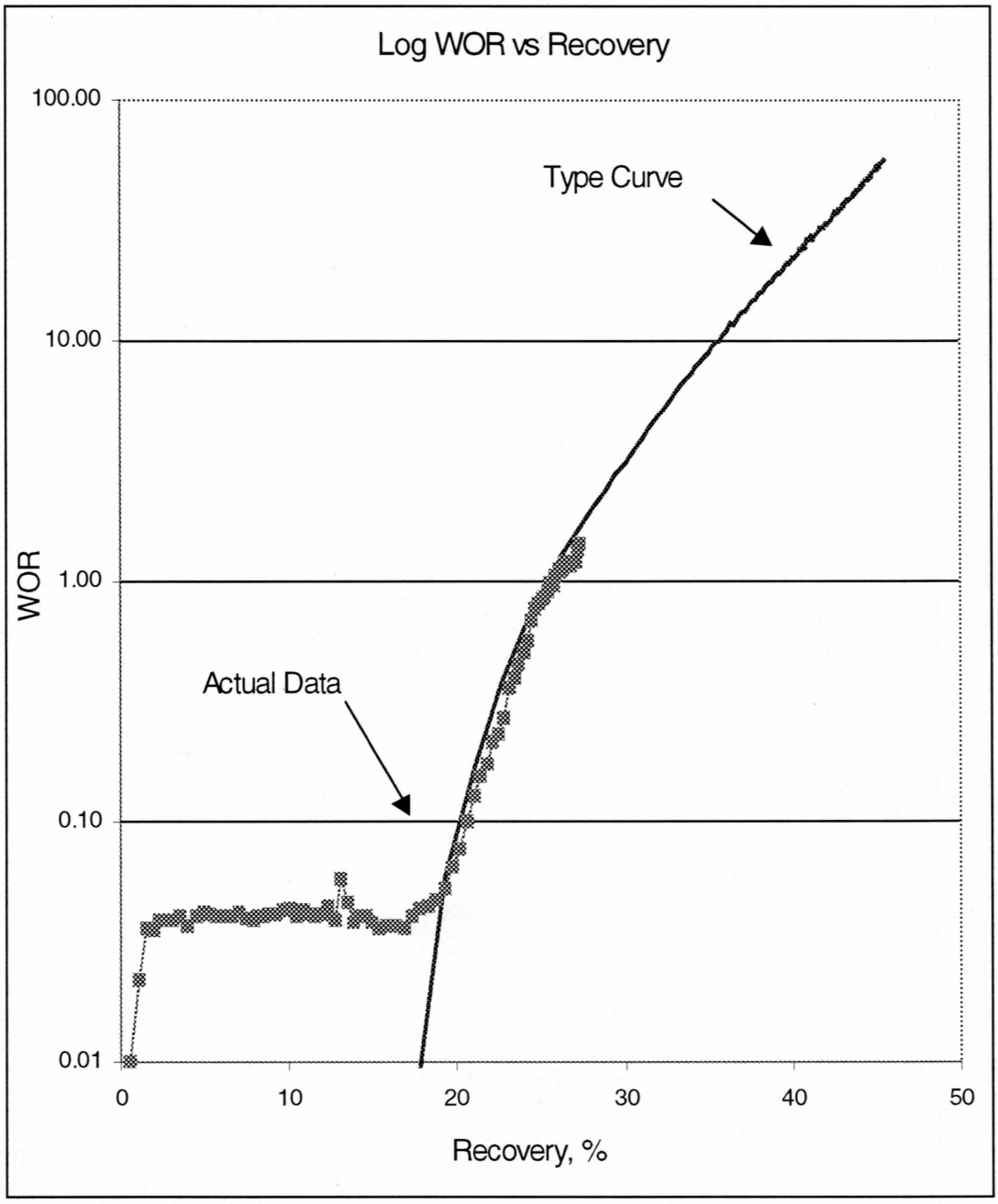

Figure 8: Actual Production Data with best fit Type Curve

area. In other words, he was unsure of the skew factor of the pattern, but he did have other data (seismic) to narrow the possible range of skew factor.

After plotting the dimensionless form of the production data, and assuming the Dykstra-Parson coefficient was 0.9, he adjusted the skew factor to get a good type curve match. This led to the conclusion that the poorly flooded area was about 15% of well flooded area. Once this history match was achieved, he had an excellent prediction of future water cut behavior and ultimate recovery.

When using this procedure to history match a pattern's performance, the issue of non-unique solutions must be addressed. Because skew factor and permeability variation have similar effects on water cut behavior (i.e. a skewed pattern or large permeability contrast will cause early breakthrough and lower recovery), there will be more than one combination of reservoir quality, skew factor, and permeability variation that will match the production history. This is why site specific knowledge about the stratigraphy and size and shape of the pattern is so important. The engineer and geologist must use prior knowledge of core studies, log analyses, and seismic to bracket the range of uncertainty. In this example, they felt the permeability variance was very low and were relatively confident the Dykstra-Parsons coefficient was close to 0.9. Consequently, the only variable that required adjusting was skew factor, which delivered a unique solution.

It is noted that the potential error of non-unique solutions is small if breakthrough has occurred. As noted in the last observation of the previous chapter, once breakthrough has occurred (i.e. at WOR = 0.05), the range of variation for any type curve that can fit the breakthrough timing is fairly tight. Consequently, any combination of permeability variation or skew factor that fits the breakthrough timing will reasonably predict the future water cut behavior and ultimate recovery. The problem becomes one of diagnosing which factor has caused breakthrough. If is due to the stratigraphy, there may be no remedy for recovering more oil. On the other hand, if it is because the pattern is skewed, there may be an opportunity to drill a new well to recover oil from the poorly flooded area. This type of diagnosis would require more geological information, and perhaps a finely gridded finite difference model to help narrow the uncertainty.

6.2 Full-Field Forecasts by Summing Well Performance

A forecasting tool based on dimensionless recovery curves for each pattern in the field is a legitimate method of predicting full-field performance. The procedure requires an estimate of

pattern size (original oil in place) and the assignment of a type curve for each and every pattern. Once an individual well's future fluid rates can be predicted with dimensionless recovery curves and a set of throughput assumptions, the process of summing well rates and forecasting full-field performance becomes a matter of accounting.

There are several advantages of this approach. First, because an actual history match is performed for each pattern, the representation of the variation in flood performance across the field can be reasonably accurate. There are no simplifications of the reservoir description (to reduce computational time) that will tend to "homogenize" the performance prediction of individual patterns. The result is a finer resolution history match in plots such as the GOR and WOR sort (i.e. Figure 1). This tool can then be used for facility expansion evaluations with more confidence in the predicted value of additional fluid handling equipment.

Another major advantage of this type of tool, rather than one based on finite difference simulations, is the speed at which various scenarios can be run and evaluated. Obviously, the computational time to predict rates using correlations is much faster than a method based on simulation. This makes it very easy to evaluate the impacts of different development scenarios.

6.3 The Foundation for an Integrated Reservoir and Economic Evaluation Tool

One of the challenges of reservoir management is understanding what can be affected by investment level, and what cannot. All the questions about whether to drill infill wells, add compression, or fracture stimulate wells require this knowledge. A good decision maker must understand the "physics" of the system as well as the advantages and disadvantages of each option as it pertains to capital costs, maintenance costs, and risks of uncertainties.

To adequately serve this purpose, the methodology must highlight the factors that are dictated by Mother Nature, and those that can be affected by investment level. An evaluation methodology can therefore be divided into four modules: a reservoir recovery module, a throughput prediction module, a facility impacts module, and finally, the cash flow analysis module.

For such an integrated evaluation methodology to be possible, the reservoir recovery module cannot be based on a numerical model of one singular description. The evaluation methodology must represent the range of uncertainty and be able to "execute" in a very short time frame. By

describing reservoir performance with a set of dimensionless recovery curves, these objectives can be met. A more detailed explanation of each module is given below:

1. Reservoir Recovery Module – this module would be very similar to the spreadsheet program used to interpolate the results of the simulation based type curves as described earlier. Obviously the type curves would have to be specific to the reservoir and patterns that are being evaluated. In this module, the user would estimate the reservoir characteristics that define recovery performance so that a type curve for that situation could be chosen.
2. Throughput Prediction Module – this module is the part that "drives" the dimensionless recovery curves. It would require input regarding the size of pattern and all parameters necessary to estimate throughput using a Darcy equation based technique. It would require relative permeability relationships to account for changing mobilities as the flood front moves through the pattern. It would also have to have a set of simplifying assumptions so that the calculations could be performed with a spreadsheet program.
3. Facility Limits Module - this module would require an estimate of the future marginal WOR and GOR. It would then be able to estimate how much marginal oil would have to be shut-in as a result of additional oil, water, and gas production of the project being evaluated.
4. Cash Flow Analysis Module – the final module would merge the facility limited oil stream with the corresponding capital and expense costs, and the appropriate tax and financial assumptions, to calculate a present worth and rate of return.

In summary, the dimensionless recovery curves become the foundation of an integrated planning and evaluation tool. This tool allows for quick evaluations of all types of depletion strategies ranging from infill drilling to the application of electric submersible pumps. It can be based on a spreadsheet program so that sensitivity and Monte Carlo simulations can be performed to bracket the range of value given the expected range of uncertainty around individual variables. A tool like this is recommended for future work.

CHAPTER 7

SUMMARY AND CONCLUSIONS

In very large, moderately mature fields, there are alternatives to single description finite difference models to help make decisions. This work presents the advantages of the dimensionless type curve approach and describes a simulation based methodology to create such curves. A case study of a very large, waterflooded field is presented to demonstrate its utility. The methodology can be applied to many types of fields.

The case study develops and presents a set of simulation based performance curves that serve as the basis for predicting recovery over a wide range of reservoir quality, permeability variation, and pattern geometry. A spreadsheet was created to interpolate among the simulation output to predict recovery of any description within the range of input. This spreadsheet can be used in conjunction with throughput calculations to predict oil, water, and gas rates for a number of different "reservoir descriptions" in a manner that is fast enough to allow for numerous sensitivities, and/or Monte Carlo simulations. These dimensionless relationships can also be compared to actual field data, or be used to predict fluid rates of all wells in the field and serve as the basis of a full-field model.

The major conclusions of this work are listed below:

- Dimensionless recovery curves combine the best of simulation and analytical solution approaches.
- To properly define and build the type curves, the user must understand the factors that affect recovery. This includes all geologic, stratigraphic, and mechanistic factors that affect flood performance.
- The methodology is not limited to waterflooded fields. It can be applied to many types of fields as long as the factors that affect recovery are anticipated, and simulation datasets that model these factors are created and executed.
- The dimensionless relationships can be used in a number of applications including full field models, comprehensive evaluation tools, and for comparing actual production to predicted performance.

List of Cited References

1. Ershaghi, I., Omoregie, O: "A Method for Extrapolation of Cut vs. Recovery Curves". *Journal of Petroleum Technology*. February, 1978. Pp. 203-204.
3. Ershaghi, I., Abdassah, D: "A Prediction Technique for Immiscible Processes Using Field Performance Data". *Journal of Petroleum Technology*. April, 1984. Pp. 664-670.
4. Startzman, R. A., Wu C.H., "Discussion of Empirical Prediction Technique for Immiscible Processes". *Journal of Petroleum Technology*. December, 1984. Pp 2192-2194
5. Lo, K. K., Warner Jr., H. R., Johnson, J. B.: "A Study of Post-Breakthrough Characteristics of Waterfloods", SPE Paper 20064 presented at the California Regional Meeting in Ventura, CA, 4-6 April, 1990.
6. Dunn, M. D.: "A Method to Estimate the Value of Well Log Information", SPE Paper 24672 presented at the 67th Annual Technical Conference in Washington D. C., 4-7 October, 1992.
7. Muskat, M.: "The Theory of Nine-Spot Flooding Networks", *Production Monthly*. March, 1948.
8. Prats, M.: "The Breakthrough Sweep Efficiency of a Staggered Line Drive", *Trans., AIME* Vol. 207, 1956. Pp 361-362.
9. Craig, F. F. Jr., "Effect of Permeability Variation and Mobility Ratio on Five-Spot Oil Recovery Performance Calculations", *Journal of Petroleum Technology*, October 1970. Pp 1239-1245.
10. Dykstra, H. and Parsons, R. L.: "The Prediction of Waterflood Performance with Variation in Permeability Profile", Production Monthly (1950) 15, pp 9-12.

Uncited References

Alpay, O. A.: "A Practical Approach to Defining Reservoir Heterogeniety". *Journal of Petroleum Technology.* July, 1972. Pp 841-848.

Amyx, J. W., Bass, D. M. Jr., Whiting, R. L.: *Petroleum Reservoir Engineering.* McGraw-Hill Book Company. 1960.

Boggs, S. Jr.: *Principles of Sedimentology and Stratigraphy – Second Edition.* Prentice-Hall Books. 1995.

Ciammetti, G., Ringrose, P. S., Good, T. R., Lewis, J. M. L., and Sorbie, K. S.: "Waterflood Recovery and Fluid Flow Upscaling in a Shallow Marine and Fluvial Sandstone Sequence". SPE Paper 30783 presented at the SPE Annual Technical Conference in Dallas, TX. 22-25 Oct., 1995.

Chapman, L. R., and Thompson, R. R.: "Waterflood Surveillance in the Kuparuk River Unit Using Computerized Pattern Analysis". SPE Paper 17429 presented at the SPE California Regional Meeting in Long Beach, CA. 23-25 March, 1998.

Coats, K. H.: "Use and Misuse of Reservoir Simulation Models". *Journal of Petroleum Technology.* November 1969. Pp 1391-1398.

Craft, B. C., Hawkins, M., Terry, R. E. *Applied Petroleum Reservoir Engineering Second Edition.* Prentice Hall, 1990.

Craig, F. F. Jr.: *The Reservoir Engineering Aspects of Waterflooding.* AIME, Third Printing, 1980.

Crichlow, H. B.: *Modern Reservoir Engineering, A Simulation Approach.* Prentice-Hall Inc. 1977.

Currier, J. H., and Sindelar, S. T.: "Performance Analysis in an Immature Waterflood: The Kuparuk River Field" SPE paper 20775 presented at the 65th Annual Technical Conference in New Orleans, LA. 23-26 September, 1990.

Dake, L. P., *Fundamentals of Reservoir Engineering.* Elsevier Scientific Publishing Company, 1978.

Dunn, M. D., Lagerlef, D. L., and Chamberlain, J. A.: "Gas Management in a Large, Complex, Miscibly Flooded Oil Field, SPE Paper 59413 to be presented at the SPE Asia-Pacific Conference on Integrated Modelling for Asset Management in Yokohama, Japan, 25-26 April 2000.

Fanchi, J. R.: *Applied Reservoir Simulation.* Gulf Publishing. 1997.

Mattax, C. C., Dalton, R. L.: *Reservoir Simulation.* Monograph Volume 13 SPE. 1990

McCain, W. D. Jr.: *The Properties of Petroleum Fluids.* Pennwell Books, 1973.

Satter, A. and Thakur, G.: Integrated Petroleum Reservoir Management. Pennwell Books. 1994.

Staggs, H. M., Herbeck, E. F.: "Reservoir Simulation Models – An Engineering Overview". Journal of Petroleum Technology. December, 1971. Pp 1428-1436.

Starley, G. P., Masino, W. H. Jr., Weiss, J. L., and Bolling, J. D.: "Full-Field Simulation for Development Planning and Reservoir Management at the Kuparuk River Field". *Journal of Petroleum Technology.* August 1991. Pp 974-982.

Walker, R. G., James, N. P.: *Facies Models – Response to Sea Level Change.* Geological Association of Canada. 1992.

Wiggins, M. L., Startzman, R. A.: "An Approach to Reservoir Management", SPE Paper 20747 presented at the 65th Annual Technical Conference in New Orleans, LA. 23-26 September, 1990.

Willhite, G. P.: *Waterflooding.* SPE Textbook Series Vol. 3 1986.

Wolcott, D. S., and Chopra, A. K.: "Incorporating Reservoir Hetrogeneity Using Geostatistics to Investigate Waterflood Recoveries for Drillsite 1E, A4 Sandstone Body, Kuparuk River Field, Alaska". SPE Paper 22164 presented at the International Arctic Technology Conference in Anchorage, AK. 29-31 May, 1991.

Wu, C. H. "Waterflood Performance Projection Using Classical Waterflood Models", SPE Paper 18597 presented at the SPE Production Technology Symposium in Hobbs, NM. 7-8 November, 1988.

Appendix A: Sample Simulation Dataset

```
; sf13idp7fair
; Skew Factor 1.33, Injector skewed, Dykstra-Parsons .7, fair continuity
; This dataset represents a pattern with skew factor 1.33p (moderately skewed near injector),
; a Dykstra-Parsons (Variance) coefficient of 0.7, with "fair" permeability and continuity,
; This would be a pattern with a fault about 1/3 away from an injector, moderate permeability
; variation,
;
; and stratigraphy of limited flaser bed, some laminated HCS, and some amalgamated HCS beds.
;
; The simulation is based on a line drive pattern with injectors on both sides of a producer.
; Kv:Kh ratio is low at 0.001. Reservoir Continuity is 90%. Discontinuity is represented
; by a transmissibility barrier halfway between injector and producer to allow for some
; "primary" production from discontinuous sands. The discontinuous sands are encased in shale.
;
; This is part of a large study to quantify the waterflood performance of different A sand
; descriptions and pattern geometries. This study consists of 45 datasets to represent the effect
; of three primary factors: Pattern geometry (skew factor, producer or injector skewed),
; Continuity, and Permeability Variance (Dykstra-Parsons coefficient).
;
; The 45 datasets account for all combinations of 6 pattern shapes (skew factors 1.0, 1.33, 1.67,
; producer or injector skewed), 3 levels of continuity (good, fair, poor), and 3 levels of
; permeability variation (Dyksta-Parsons coefficient of 0.9, 0.7, 0.5).
;
; Created by:    Mike Dunn
; Creation Date: 2-7-2000
; Revision Date: 2-7-2000
;*************************************************************************
;
; SECTIONS
;
; Grid Definition          p. 1
; Fluid Properties         p. 1-2
; Saturation Functions     p. 2-5
; Reservoir Description    p. 5
; Edge Cell Modifiers      p. 6
; Miscellaneous Initial Data  p. 6
; Recurrent Data           p. 6
; Well Data                p. 6-7
; Time Step Controls       p. 7
;
 TITLE Skew Factor 1.33, Producer skewed, Moderate Perm Variance, Fair continuity,
;
;
; Element of symmetry: one-quarter of 320 acre pattern with injector near left corner (7,1),
;
; and producer in top right corner (24,1) and a barrier 1/3 to left of injector (1,1-9)
; This is 160 acre well spacing, or 4 wells per sq. mile.
; 24 X 9 (216) grids that are roughly 1/2 acre each
; 12 layers or flow units in the z direction for total of 2592 cells.
;
 USERID   M. D. Dunn
;
 DATE     2/8/2000
; First created 2/7/2000
 BINARY
;
;*************************************************************************
; Grid Definition Section
;*************************************************************************
;
; Grid is designed to have ~1/2 acre cells in the xy direction
; The z direction is setup with 12 layers for 35' of net pay
```

```
; The "flow units" are not based on a specific core but are somewhat arbitrary
NX 24  NY 9  NZ 12
DX XVAR 24*147
DY YVAR 9*147
DZ ZVAR 2 3 4 2 3 5 1.5 2 2.5 4 2 4
;
;*****************************************************************************
; Fluid Properties Section
;*****************************************************************************
WOG
DENWB   63.946  ; STANDARD WATER DENSITY (LB/FT3)
API     22      ; KUPARUK CRUDE DENSITY
SPECG   .75     ; KUPARUK GAS DENSITY
BW      0.99006 ; WATER FORMATION VOLUME FACTOR (RVB/STB)
CW      3.3     ; WATER COMPRESSIBILITY (VOL/MVOL/PSI)
VISW    0.50    ; WATER VISCOSITY (CP)
TRES    160     ; TEMPERATURE OF THE RESERVOIR
;
; PVT PROPERTIES BASED ON GENERIC WELL AT 6000' SS
; BUBBLE POINT OF 2637 psia, 22 API
;
PVT   NBP 12    CO 23.2
      PT     BOT     BGT     RST     VOT     VGT
;    psia   rvb/stb  rvb/mcf  mcf/stb   cp      cp
;   ------  -------  -------  -------  -----   -----
      15    1.010   180.000   .0001    9.14    0.0098
     168    1.049    16.667   .056     6.80    0.0117
     365    1.067     8.333   .099     5.30    0.0125
     615    1.083     5.000   .141     4.58    0.0131
     865    1.097     3.333   .181     4.10    0.0137
    1115    1.112     2.597   .221     3.70    0.0143
    1365    1.125     2.083   .259     3.38    0.0148
    1615    1.140     1.724   .299     3.10    0.0155
    1865    1.154     1.471   .337     2.80    0.0162
    2115    1.169     1.282   .376     2.56    0.0170
    2365    1.182     1.143   .414     2.32    0.0178
    2637    1.198     1.020   .455     2.09    0.0188
    3015    1.219     0.883   .513     1.79    0.0204
    4015    1.276     0.655   .670     0.93    0.0241
    5015    1.333     0.520   .825     0.51    0.0278
;
;*****************************************************************************
; Saturation Functions (Rel Perm)
;*****************************************************************************
;
;
; Z sand oil, gas, and water rel perm function parameters
;
;
A90WO    TABLE 1  SWI      0.15      ; PRIMARY IMBIBITION
SW       KRWO     KROW      PCWO
0.0000   0.000E+00 1.000E+00 6.595E+00
0.0208   1.630E-05 8.641E-01 4.194E+00
0.0416   1.508E-04 7.438E-01 2.625E+00
0.0623   5.539E-04 6.377E-01 1.597E+00
0.0831   1.394E-03 5.445E-01 9.300E-01
0.1039   2.850E-03 4.628E-01 5.058E-01
0.1247   5.108E-03 3.915E-01 2.468E-01
0.1454   8.358E-03 3.296E-01 9.986E-02
0.1662   1.279E-02 2.759E-01 2.754E-02
0.1870   1.858E-02 2.298E-01 2.242E-03
0.2078   2.591E-02 1.902E-01 -4.920E-02
0.2285   3.494E-02 1.564E-01 -1.007E-01
0.2493   4.581E-02 1.277E-01 -1.393E-01
0.2701   5.863E-02 1.035E-01 -1.733E-01
0.2909   7.351E-02 8.327E-02 -2.050E-01
```

```
0.3116   9.048E-02 6.641E-02 -2.356E-01
0.3324   1.096E-01 5.247E-02 -2.656E-01
0.3532   1.308E-01 4.105E-02 -2.956E-01
0.3740   1.541E-01 3.176E-02 -3.259E-01
0.3947   1.793E-01 2.428E-02 -3.568E-01
0.4155   2.064E-01 1.833E-02 -3.887E-01
0.4363   2.352E-01 1.363E-02 -4.217E-01
0.4571   2.654E-01 9.978E-03 -4.563E-01
0.4778   2.970E-01 7.175E-03 -4.927E-01
0.4986   3.297E-01 5.057E-03 -5.315E-01
0.5194   3.631E-01 3.485E-03 -5.729E-01
0.5402   3.972E-01 2.340E-03 -6.177E-01
0.5609   4.317E-01 1.526E-03 -6.666E-01
0.5817   4.663E-01 9.616E-04 -7.203E-01
0.6025   5.008E-01 5.820E-04 -7.802E-01
0.6233   5.351E-01 3.358E-04 -8.478E-01
0.6440   5.690E-01 1.828E-04 -9.253E-01
0.6648   6.022E-01 9.267E-05 -1.016E+00
0.6856   6.347E-01 4.289E-05 -1.124E+00
0.7064   6.664E-01 1.762E-05 -1.257E+00
0.7271   6.971E-01 6.154E-06 -1.427E+00
0.7479   7.269E-01 1.698E-06 -1.657E+00
0.7687   7.555E-01 3.229E-07 -1.995E+00
0.7895   7.831E-01 3.112E-08 -2.567E+00
0.8102   8.095E-01 5.703E-10 -3.889E+00
0.8310   8.347E-01 0.000E+00 -8.000E+00
1.0000   1.000E+00 0.000E+00 -2.000E+01
;
A90WO    TABLE 1  SWI      0.5
SW       KRWO     KROW     PCWO
0.0000   0.000E+00 1.000E+00 3.997E-01
0.0208   1.630E-05 8.641E-01 3.593E-01
0.0416   1.508E-04 7.438E-01 3.224E-01
0.0623   5.539E-04 6.377E-01 2.886E-01
0.0831   1.394E-03 5.445E-01 2.577E-01
0.1039   2.850E-03 4.628E-01 2.295E-01
0.1247   5.108E-03 3.915E-01 2.038E-01
0.1454   8.358E-03 3.296E-01 1.804E-01
0.1662   1.279E-02 2.759E-01 1.591E-01
0.1870   1.858E-02 2.298E-01 1.398E-01
0.2078   2.591E-02 1.902E-01 1.224E-01
0.2285   3.494E-02 1.564E-01 1.066E-01
0.2493   4.581E-02 1.277E-01 9.237E-02
0.2701   5.863E-02 1.035E-01 7.959E-02
0.2909   7.351E-02 8.327E-02 6.814E-02
0.3116   9.048E-02 6.641E-02 5.793E-02
0.3324   1.096E-01 5.247E-02 4.885E-02
0.3532   1.308E-01 4.105E-02 4.081E-02
0.3740   1.541E-01 3.176E-02 3.374E-02
0.3947   1.793E-01 2.428E-02 2.756E-02
0.4155   2.064E-01 1.833E-02 2.220E-02
0.4363   2.352E-01 1.363E-02 1.759E-02
0.4571   2.654E-01 9.978E-03 1.366E-02
0.4778   2.970E-01 7.175E-03 1.035E-02
0.4986   3.297E-01 5.057E-03 7.615E-03
0.5194   3.631E-01 3.485E-03 5.392E-03
0.5402   3.972E-01 2.340E-03 3.631E-03
0.5609   4.317E-01 1.526E-03 2.283E-03
0.5817   4.663E-01 9.616E-04 1.298E-03
0.6025   5.008E-01 5.820E-04 6.291E-04
0.6233   5.351E-01 3.358E-04 2.269E-04
0.6440   5.690E-01 1.828E-04 3.893E-05
0.6648   6.022E-01 9.267E-05 -3.535E-02
0.6856   6.347E-01 4.289E-05 -1.922E-01
0.7064   6.664E-01 1.762E-05 -3.065E-01
```

```
0.7271   6.971E-01 6.154E-06 -4.263E-01
0.7479   7.269E-01 1.698E-06 -5.690E-01
0.7687   7.555E-01 3.229E-07 -7.604E-01
0.7895   7.831E-01 3.112E-08 -1.062E+00
0.8102   8.095E-01 5.703E-10 -1.722E+00
0.8310   8.347E-01 0.000E+00 -8.000E+00
1.0000   1.000E+00 0.000E+00 -2.000E+01
;
A90WO    TABLE 1  SWI      1.0
SW       KRWO     KROW     PCWO
0.0000   0.000E+00 1.000E+00 1.000E+02
0.0020   2.768E-26 1.000E+00 1.000E+02
0.0050   1.732E-22 1.000E+00 1.000E+02
0.0070   4.291E-21 9.999E-01 1.000E+02
0.0100   1.289E-19 9.998E-01 1.000E+02
0.0200   9.597E-17 9.994E-01 1.000E+02
0.0300   4.593E-15 9.986E-01 1.000E+02
0.0400   7.145E-14 9.974E-01 6.505E+01
0.0600   3.419E-12 9.941E-01 3.395E+01
0.0800   5.319E-11 9.892E-01 2.092E+01
0.1000   4.470E-10 9.828E-01 1.413E+01
0.1200   2.545E-09 9.748E-01 1.012E+01
0.1400   1.108E-08 9.650E-01 7.547E+00
0.1600   3.959E-08 9.535E-01 5.802E+00
0.1800   1.218E-07 9.402E-01 4.566E+00
0.2000   3.328E-07 9.250E-01 3.659E+00
0.2200   8.261E-07 9.081E-01 2.978E+00
0.2400   1.895E-06 8.892E-01 2.454E+00
0.2600   4.066E-06 8.685E-01 2.044E+00
0.2800   8.246E-06 8.460E-01 1.719E+00
0.3000   1.592E-05 8.217E-01 1.458E+00
0.3200   2.948E-05 7.958E-01 1.246E+00
0.3400   5.256E-05 7.682E-01 1.072E+00
0.3600   9.067E-05 7.391E-01 9.283E-01
0.3800   1.519E-04 7.087E-01 8.089E-01
0.4000   2.477E-04 6.770E-01 7.090E-01
0.4200   3.946E-04 6.443E-01 6.251E-01
0.4400   6.150E-04 6.107E-01 5.542E-01
0.4600   9.398E-04 5.763E-01 4.942E-01
0.4800   1.411E-03 5.415E-01 4.431E-01
0.5000   2.082E-03 5.063E-01 3.997E-01
0.5200   3.027E-03 4.710E-01 3.626E-01
0.5400   4.339E-03 4.357E-01 3.309E-01
0.5600   6.138E-03 4.008E-01 3.038E-01
0.5800   8.579E-03 3.664E-01 2.805E-01
0.6000   1.185E-02 3.326E-01 2.606E-01
0.6200   1.621E-02 2.997E-01 2.436E-01
0.6400   2.194E-02 2.678E-01 2.291E-01
0.6600   2.943E-02 2.372E-01 2.166E-01
0.6800   3.913E-02 2.080E-01 2.061E-01
0.7000   5.159E-02 1.803E-01 1.971E-01
0.7200   6.749E-02 1.542E-01 1.895E-01
0.7400   8.765E-02 1.300E-01 1.831E-01
0.7600   1.130E-01 1.077E-01 1.777E-01
0.7800   1.447E-01 8.733E-02 1.733E-01
0.8000   1.842E-01 6.910E-02 1.696E-01
0.8200   2.328E-01 5.304E-02 1.666E-01
0.8400   2.923E-01 3.920E-02 1.642E-01
0.8600   3.642E-01 2.759E-02 1.623E-01
0.8800   4.499E-01 1.821E-02 1.609E-01
0.9000   5.495E-01 1.100E-02 1.598E-01
0.9200   6.610E-01 5.829E-03 1.590E-01
0.9400   7.779E-01 2.512E-03 1.585E-01
0.9600   8.872E-01 7.405E-04 1.582E-01
0.9800   9.688E-01 8.616E-05 1.580E-01
```

```
1.0000    1.000E+00 0.000E+00 1.580E-01
;
;
;*****************************************************************************
; Reservoir Description (Rock Properties)
;*****************************************************************************
;
;  Reservoir description is "generic fair Z sand" with some amalgamated HCS beds
;  There is no directional permeability difference in the xy direction.
;  Sands are moderately laminated with thin mudstones, much like one would find in
;  in the base of sequence I and sequence II deposits.
;  Porosity varies by layer, Weighted Average Porosity is 0.22
;  Kv:Kh ratio is 0.001 to represent mudstone micro-layers.
;  Total kh is 2800.  Weighted average permeability is 80 md.
;  Permeability Variation (Dykstra-Parsons coefficient) is fair at 0.7.
;  Note:  This description is not based on a specific core - it is an arbitrary
;  "generic" description designed to represent one type of well in the continuum of
;  variation seen in Z sand descriptions.
;
 PERMX ZVAR 30 160 60 15 190 75 20 15 30 180 5 45
 KY/KX  1.0
 KZ/KX  0.001
 POR ZVAR .17 .23 .25 .19 .21 .26 .20 .21 .24 .23 .20 .18
;  In this case, 160 acre well spacing, layers 7, 8 are discontinuous
;  about halfway in the x direction between the injector and producer
;  These layers are completely encased in shale with permz = 0.
;  This is equivalent to 90% continuity
 BARRIERS X+ RESET
 BARRIERS X+
 VALUE  IX1  IX2  JY1  JY2  KZ1  KZ2
  0     15   15   1    9    7    7
 BARRIERS X+
 VALUE  IX1  IX2  JY1  JY2  KZ1  KZ2
  0     15   15   1    9    8    8
 MOD MULTIPLY PERMZ
  VALUE        IX1  IX2  JY1  JY2  KZ1  KZ2
   0.0          1    24   1    9    7    7
   0.0          1    24   1    9    8    8
;
;*****************************************************************************
; Edge Cell Modifiers to account for boundaries around this pattern
;*****************************************************************************
;
;
 MOD MULTIPLY PV
  VALUE        IX1  IX2  JY1  JY2  KZ1  KZ2
   0.5          1    24   1    1    1    12  ;--- NORTH
   0.5          1    24   9    9    1    12  ;--- SOUTH
   0.5          1    1    1    9    1    12  ;--- WEST
   0.5         24    24   1    9    1    12  ;--- EAST
;
 MOD MULTIPLY TZ
  VALUE        IX1  IX2  JY1  JY2  KZ1  KZ2
   0.5          1    24   1    1    1    12  ;--- NORTH
   0.5          1    24   9    9    1    12  ;--- SOUTH
   0.5          1    1    1    9    1    12  ;--- WEST
   0.5         24    24   1    9    1    12  ;--- EAST
;
 MOD MULTIPLY TX
  VALUE        IX1  IX2  JY1  JY2  KZ1  KZ2
   0.5          1    24   1    1    1    12  ;--- NORTH
   0.5          1    24   9    9    1    12  ;--- SOUTH
;
 MOD MULTIPLY TY
  VALUE        IX1  IX2  JY1  JY2  KZ1  KZ2
   0.5          1    1    1    9    1    12  ;--- WEST
```

```
 0.5          24   24   1    9    1    12  ;--- EAST
;
;*************************************************************************
; Miscellaneous Data Section
;*************************************************************************
COMPROCK  3.309
HTOP LAYER 216*6000.
WSAT CON 0.20
PRESSURE CON 3000.
;
ENDINITDATA
;
;*************************************************************************
; Recurrent Data Section
;*************************************************************************
;
; Solution methods for flow equations
IMPLICIT
;
; The Sparse Linear Algebra Package (SLAP) matrix solution technique is specified
SLAP 3
;
; Calculate HCPVI injected based on the average pattern pressure
HCPVI  PAVG  CUMULATIVE
;
;*************************************************************************
; Well Data Section
;*************************************************************************
;
;
; Wells are numbered as follows:
;
; ------1------------------2
; |                        |  For this line drive pattern with quarter symmetry,
; |                        |  wells 1 and 2 are active.
; |                        |
; --------------------------
;
;
; Since this is one-quarter of the pattern, we use wells 1 and 2 only
; With no flow boundaries assumed at the pattern boundaries
;
; Define well 1 at  7,1  perfed in all layers
; Define well 2 at 24,1  perfed in all layers
;
WELLDEF 1 NAME INJ1   IX  7    JY   1   KZ1  1   KZ2  12
WELLDEF 2 NAME PROD2  IX  24   JY   1   KZ1  1   KZ2  12
;
;
; Wells on pressure control, with set kh, rw, skin
; Note the well rate should be adjusted down to .35 of actual to represent corner well injector
; and side well producer pair.  Rates are set to be equal to reach steady state flow at
; reasonable pattern pressure.
; These are typical properties for Kuparuk A sand stimulated injector and producer
; Waterflood for 100 years
;
WELL 1 WATINJ   RATE 9999.0 BHP 4000. RW .35 SKIN -3 KH 2800
WELL 2 FLDPROD  RATE 9999.0 BHP 1500. RW .35 SKIN -3 KH 2800
PERF 1 12*0.35
PERF 2 12*0.35
;
;*************************************************************************
; Time Step Controls
;*************************************************************************
;
```

```
OUTWELL
OUTMATBAL
ECHON
;
PRTON  SUMON
PRTDT  91.25   SUMDT  91.25
DMASS .05  DTMIN .1  DTMAX 50.0  DPRES 100  DTSTART 0.1
~
;
~
TIME   36500.
~
STOP
```

Appendix B – Simulation Results, Figures 9 - 20

Figure 9: Simulation Results – Good Reservoir Quality, Recovery vs. HCPVWI. Shows entire range of waterflood performance for "Good" reservoir quality/continuity on a scale of Percent Recovery vs. Hydrocarbon Pore Volume of Water Injected (HCPVWI).

Figure 10: Simulation Results – Good Reservoir Quality, Log WOR vs. Recovery. Shows entire range of waterflood performance for "Good" reservoir quality/continuity on a scale of Log WOR vs. Percent Recovery.

Figure 11: Simulation Results – Fair Reservoir Quality, Recovery vs. HCPVWI. Shows entire range of waterflood performance for "Fair" reservoir quality/continuity on a scale of Percent Recovery vs. HCPVWI.

Figure 12: Simulation Results – Fair Reservoir Quality, Log WOR vs. Recovery. Shows entire range of waterflood performance for "Fair" reservoir quality/continuity on a scale of Log WOR vs. Percent Recovery.

Figure 13: Simulation Results – Poor Reservoir Quality, Recovery vs. HCPVWI. Shows entire range of waterflood performance for "Poor" reservoir quality/continuity on a scale of Percent Recovery vs. HCPVWI.

Figure 14: Simulation Results –Poor Reservoir Quality, Log WOR vs. Recovery. Shows entire range of waterflood performance for "Poor" reservoir quality/continuity on a scale of Log WOR vs. Percent Recovery.

Figure 15: Impact of Reservoir Quality/Continuity, Recovery vs. HCPVWI. Shows variation in waterflood performance for the three levels of reservoir quality/continuity for a Dykstra-Parsons coefficient of 0.7 and skew factor of 1.0. On a scale of Percent Recovery vs. HCPVWI.

Figure 16: Impact of Reservoir Quality/Continuity, Log WOR vs. Recovery. Shows variation in waterflood performance for the three levels of reservoir quality/continuity for a Dykstra-Parsons coefficient of 0.7 and skew factor of 1.0. On a scale of Log WOR vs. Percent Recovery.

Figure 17: Impact of Dykstra-Parsons Coefficient, Recovery vs. HCPVWI. Shows variation in waterflood performance for three levels of permeability variation for "fair" reservoir quality case and skew factor of 1.0. On a scale of Percent Recovery vs. HCPVWI.

Figure 18: Impact of Dykstra-Parsons Coefficient, Log WOR vs. Recovery. Shows variation in waterflood performance for three levels of permeability variation for "fair" reservoir quality case and skew factor of 1.0. On a scale of Log WOR vs. Percent Recovery.

Figure 19: Impact of Skew Factor, Recovery vs. HCPVWI. Shows variation in waterflood performance for 5 skew factors (pattern shapes) for "fair" reservoir quality and Dykstra-Parsons coefficient of 0.7. On a scale of Percent Recovery vs. HCPVWI.

Figure 20: Impact of Skew Factor, Log WOR vs. Recovery. Shows variation in waterflood performance for 5 skew factors (pattern shapes) for "fair" reservoir quality and Dykstra-Parsons coefficient of 0.7. On a scale of Log WOR vs. Percent Recovery

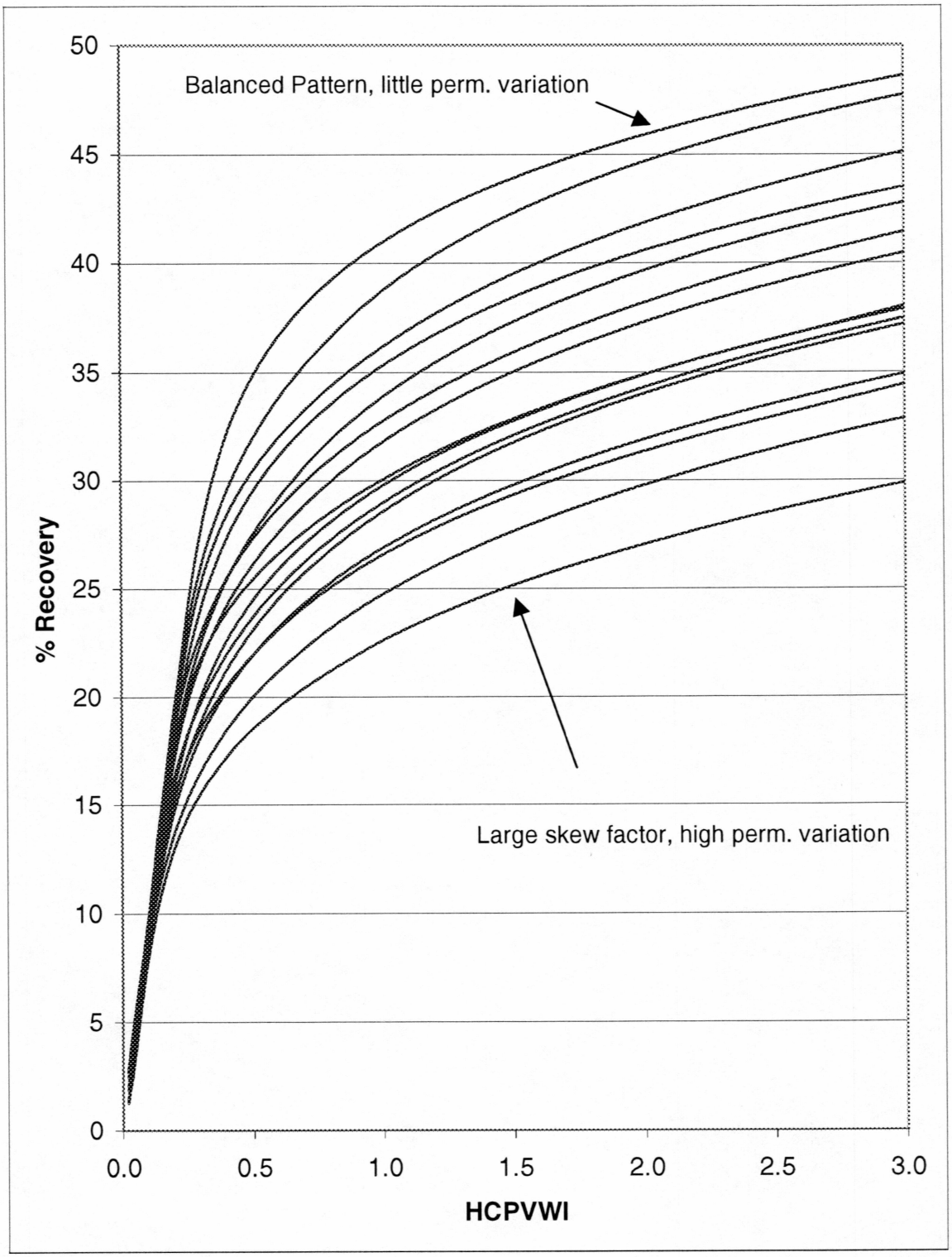

Figure 9: Simulation Results - Good Reservoir Quality, Recovery vs. HCPVWI

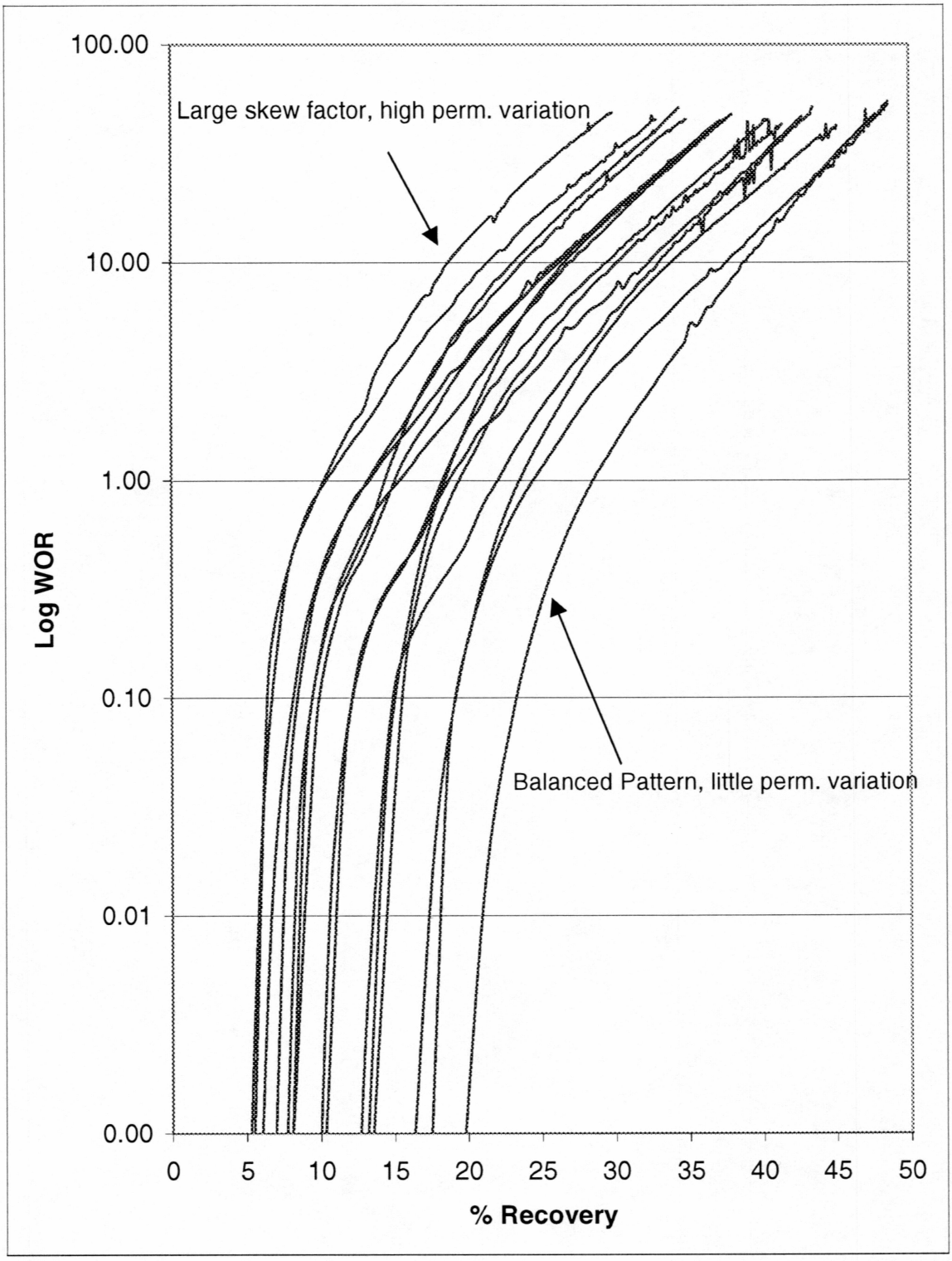

Figure 10: Simulation Results - Good Reservoir Quality, Log WOR vs. Recovery

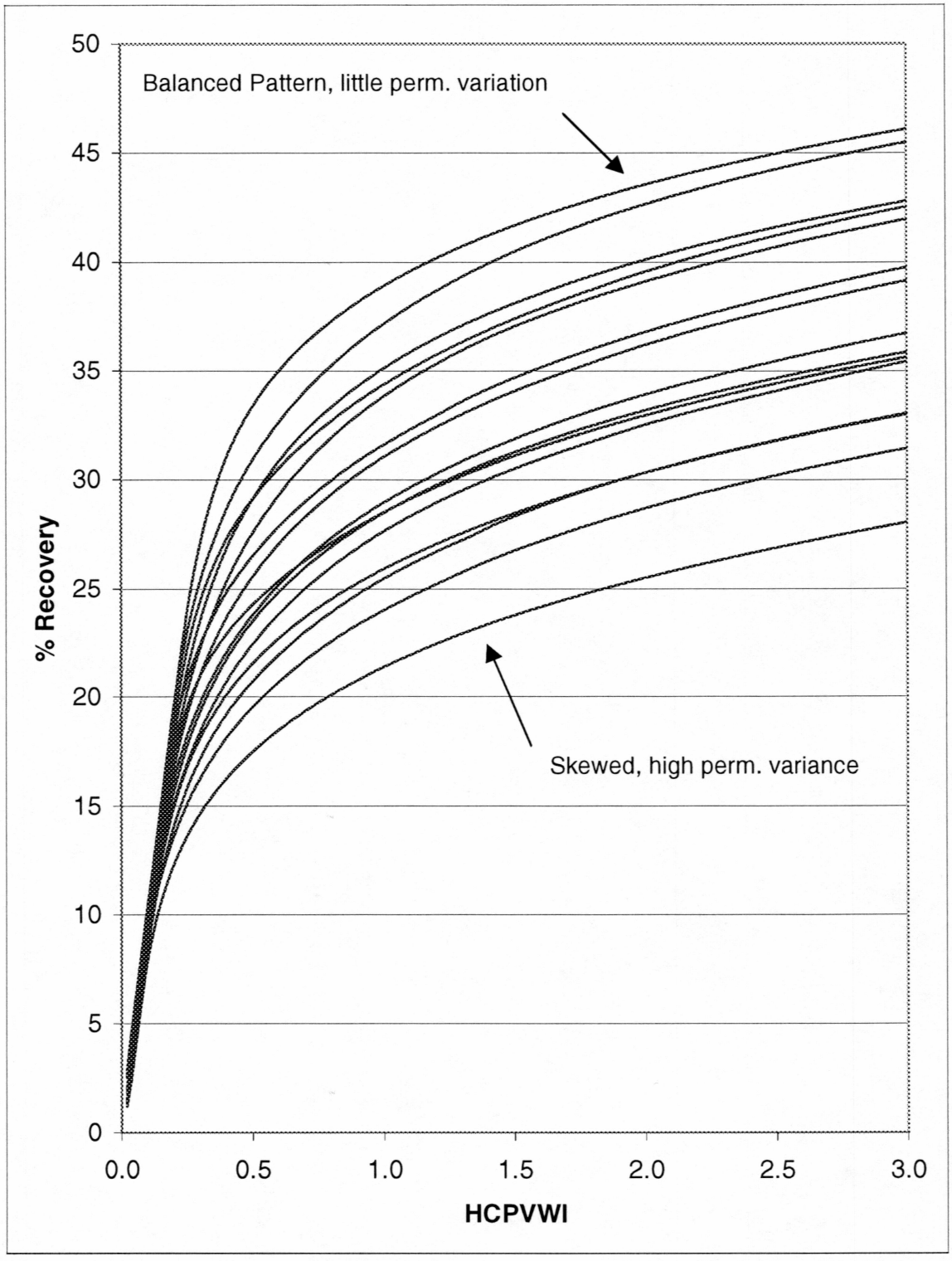

Figure 11: Simulation Results - Fair Reservoir Quality, Recovery vs. HCPVWI

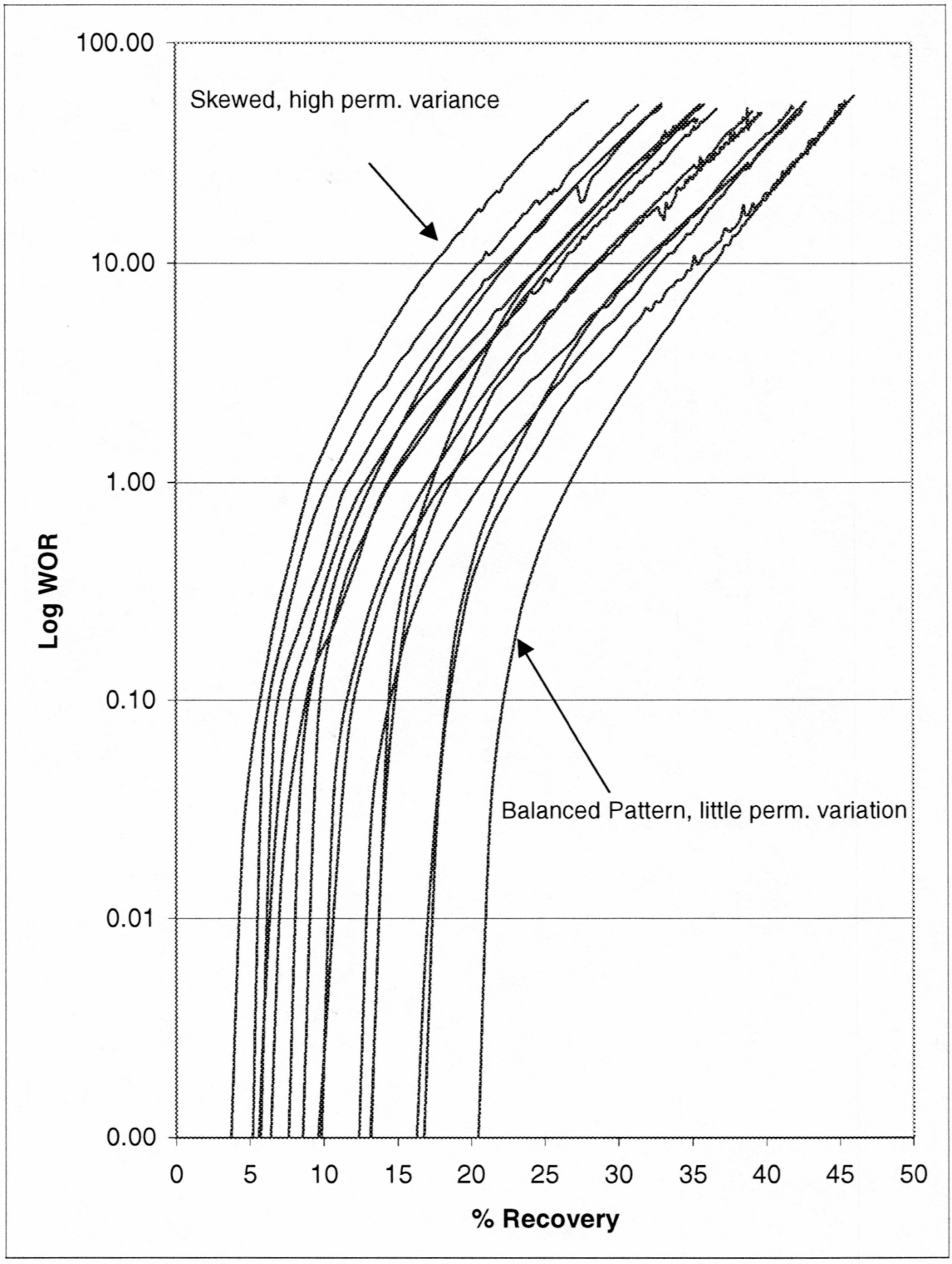

Figure 12: Simulation Results - Fair Reservoir Quality, Log WOR vs. Recovery

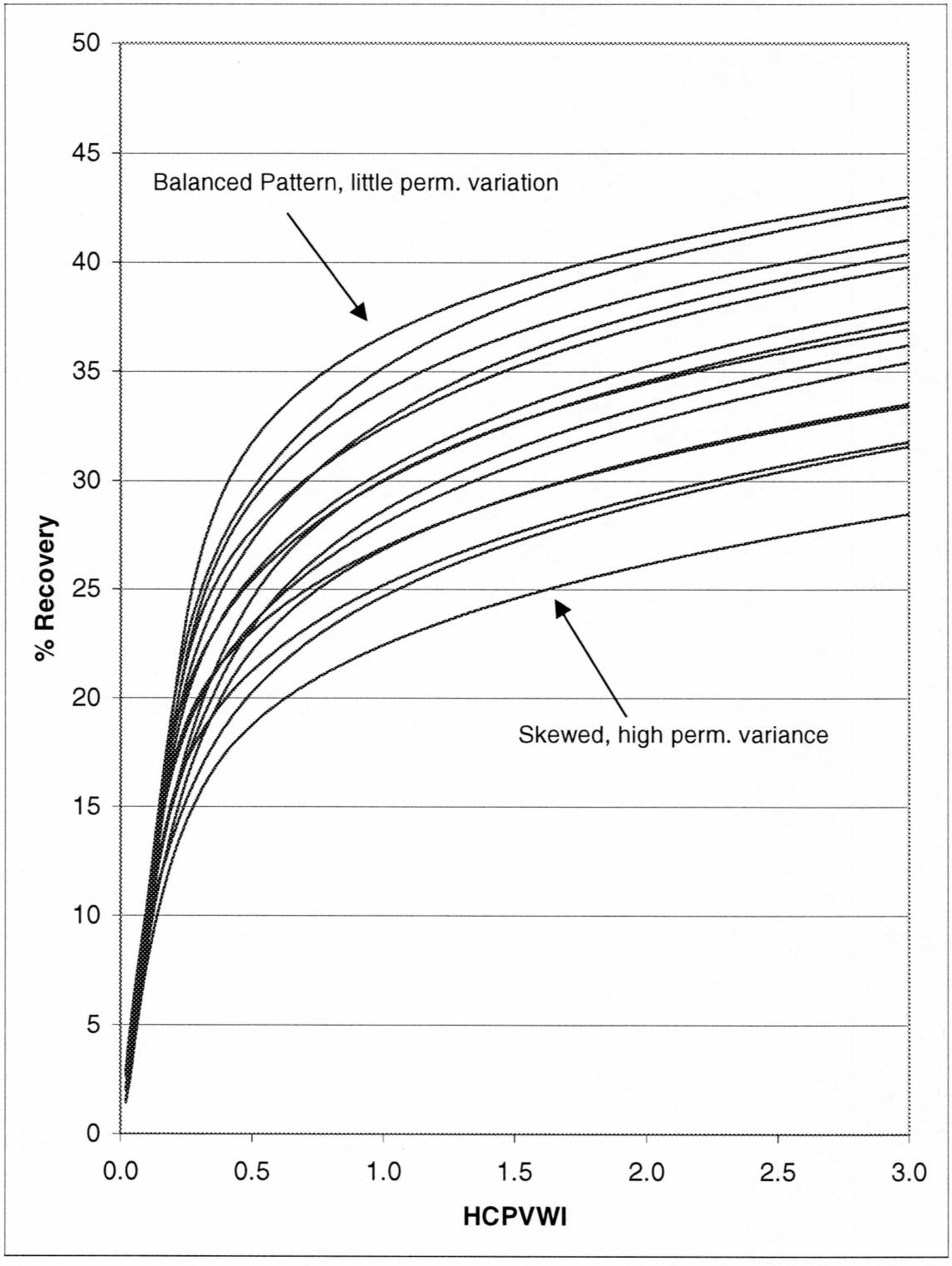

Figure 13: Simulation Results - Poor Reservoir Quality, Recovery vs. HCPVWI

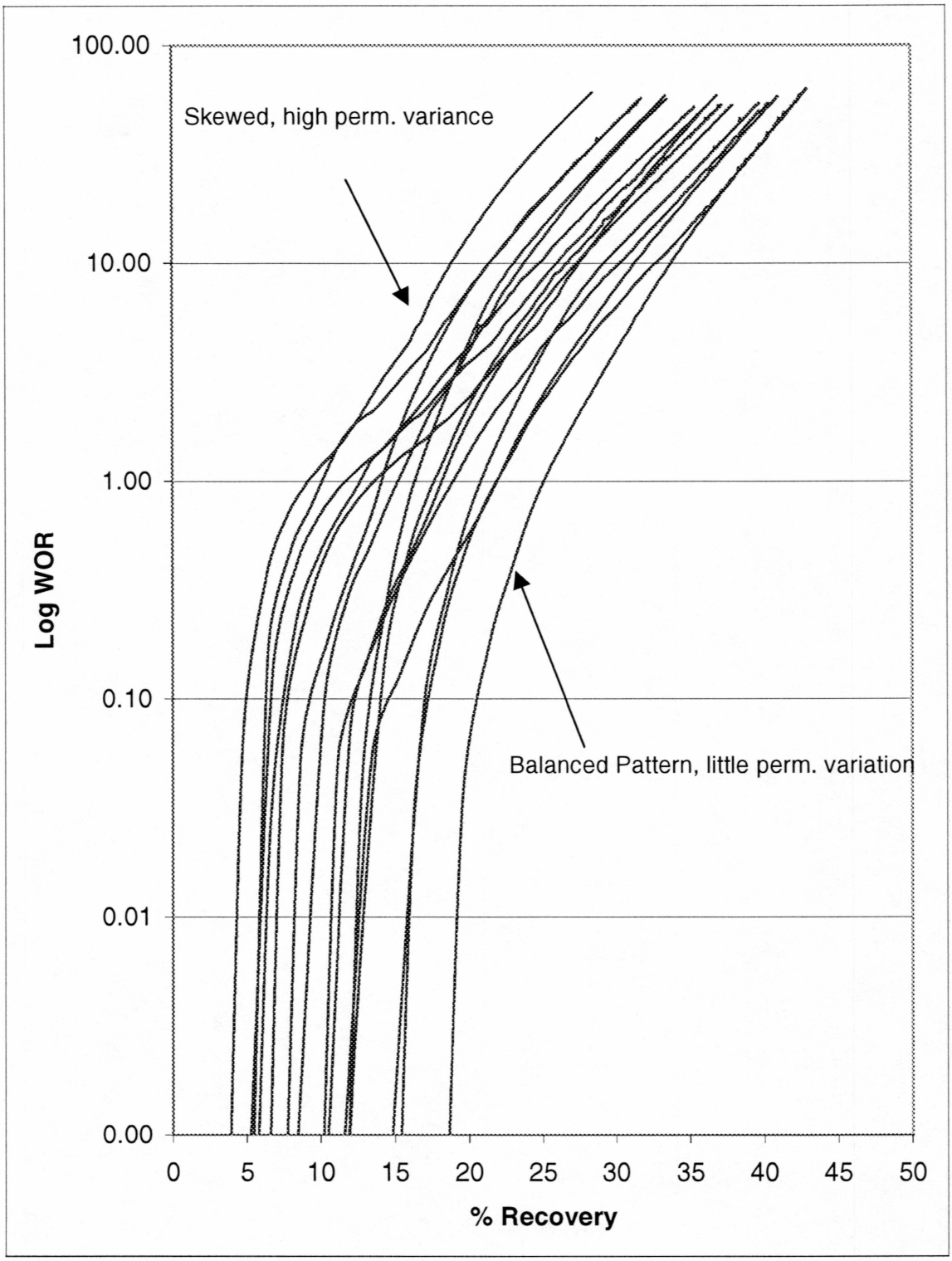

Figure 14: Simulation Results - Poor Reservoir Quality, Log WOR vs. Recovery

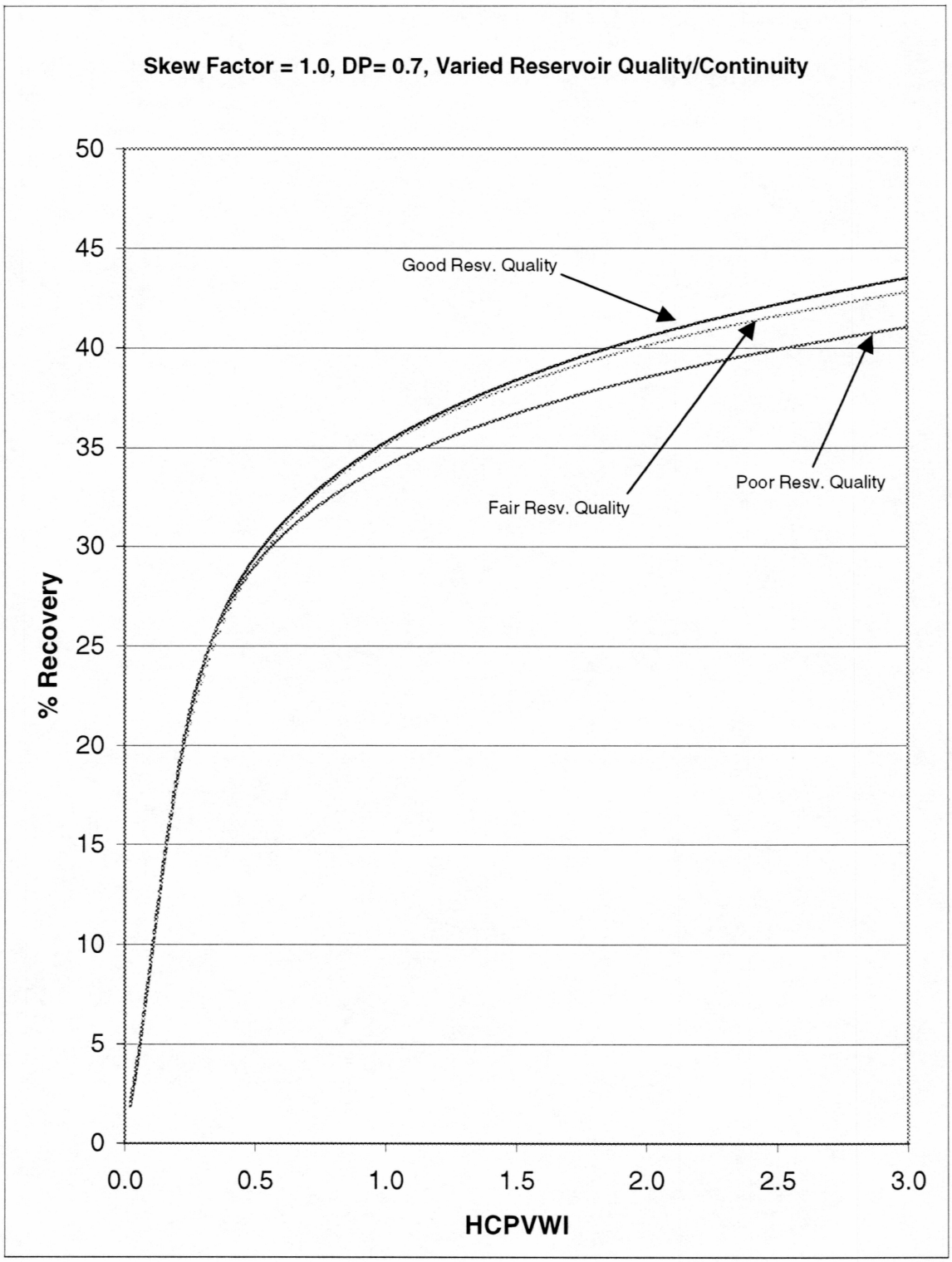

Figure 15: Impact of Reservoir Quality/Continuity - Recovery vs. HCPVWI

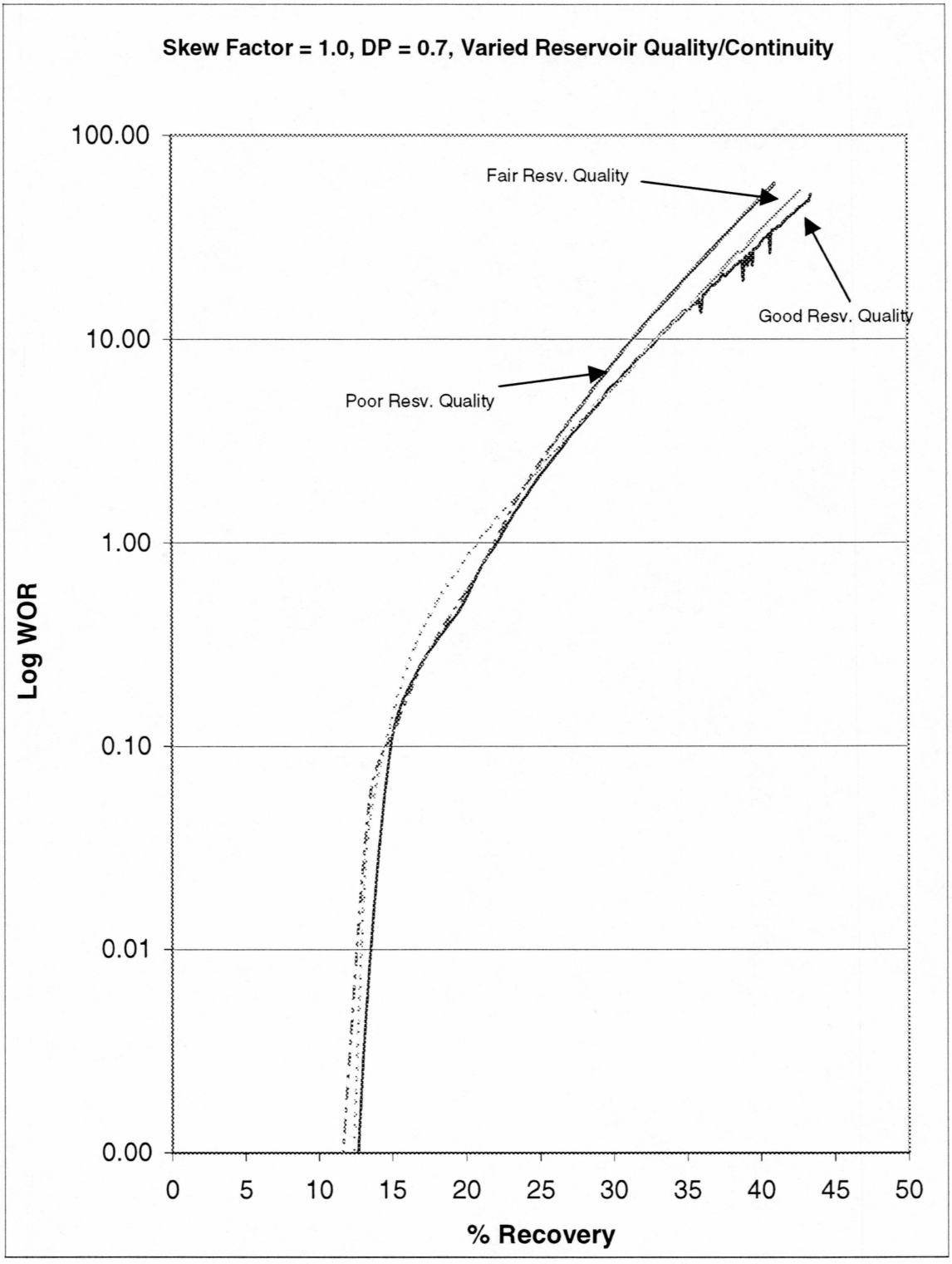

Figure 16: Impact of Reservoir Quality/Continuity - Log WOR vs. Recovery

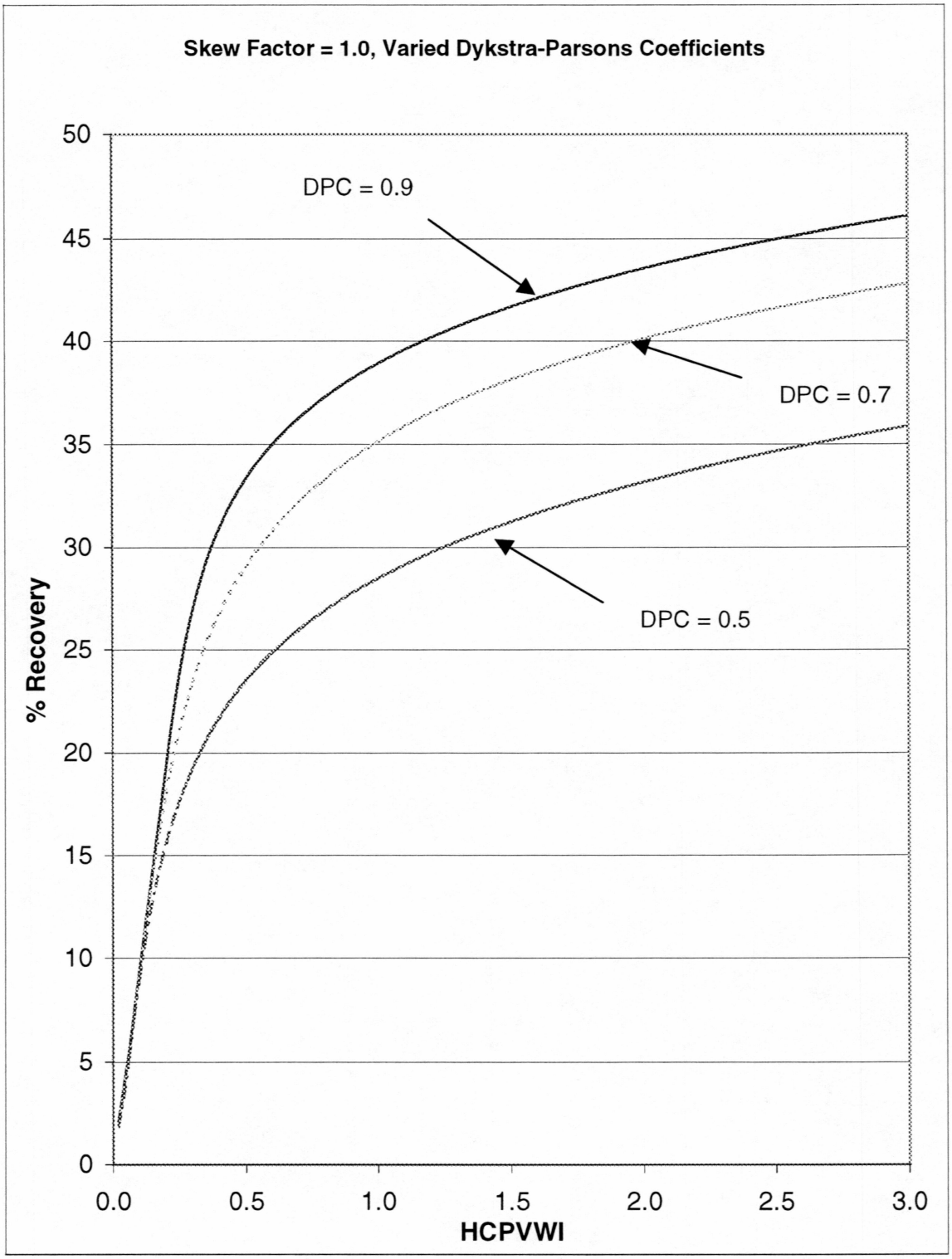

Figure 17: Impact of Dykstra-Parsons Coefficient, Recovery vs. HCPVWI

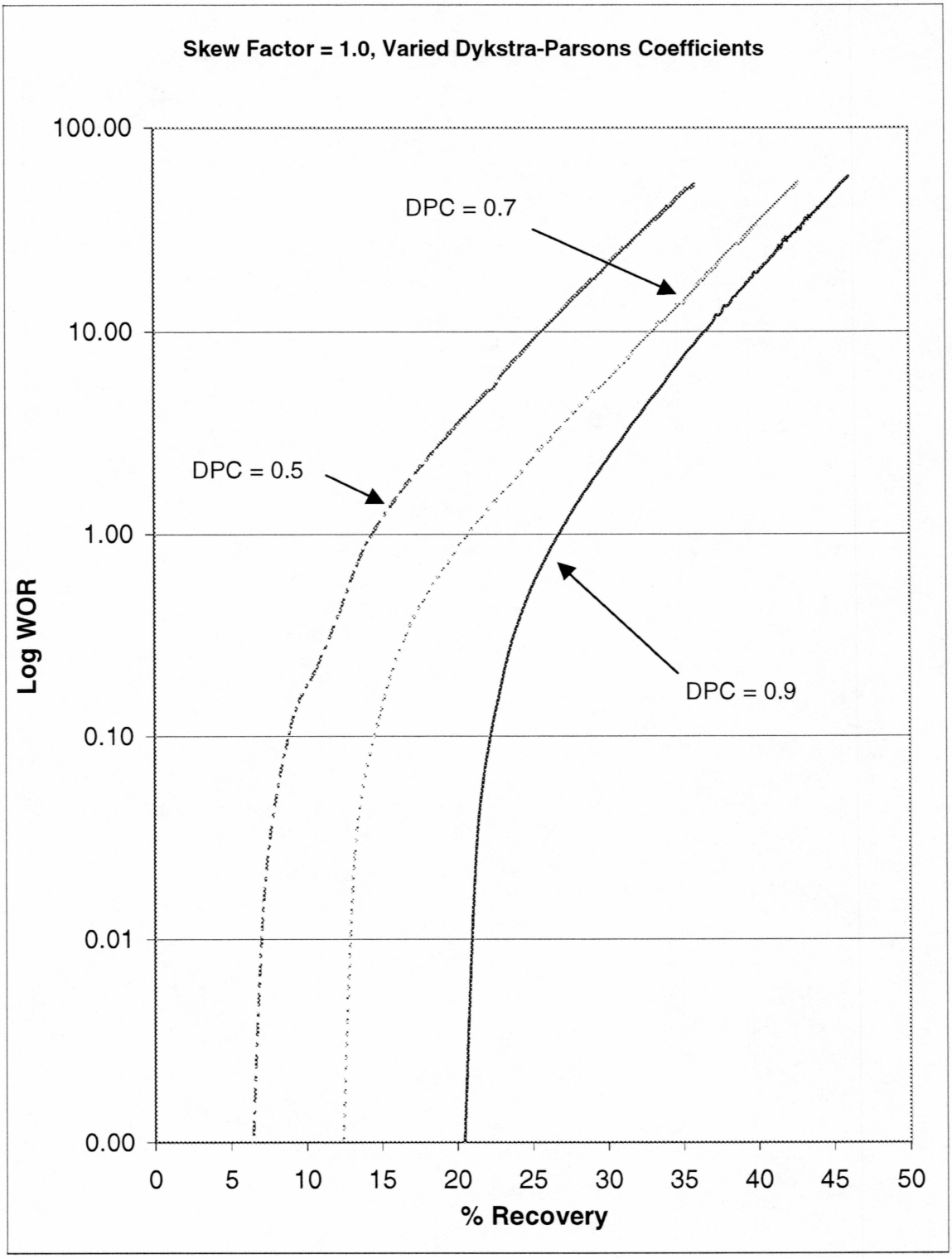

Figure 18: Impact of Dykstra-Parsons Coefficient, Log WOR vs. Recovery

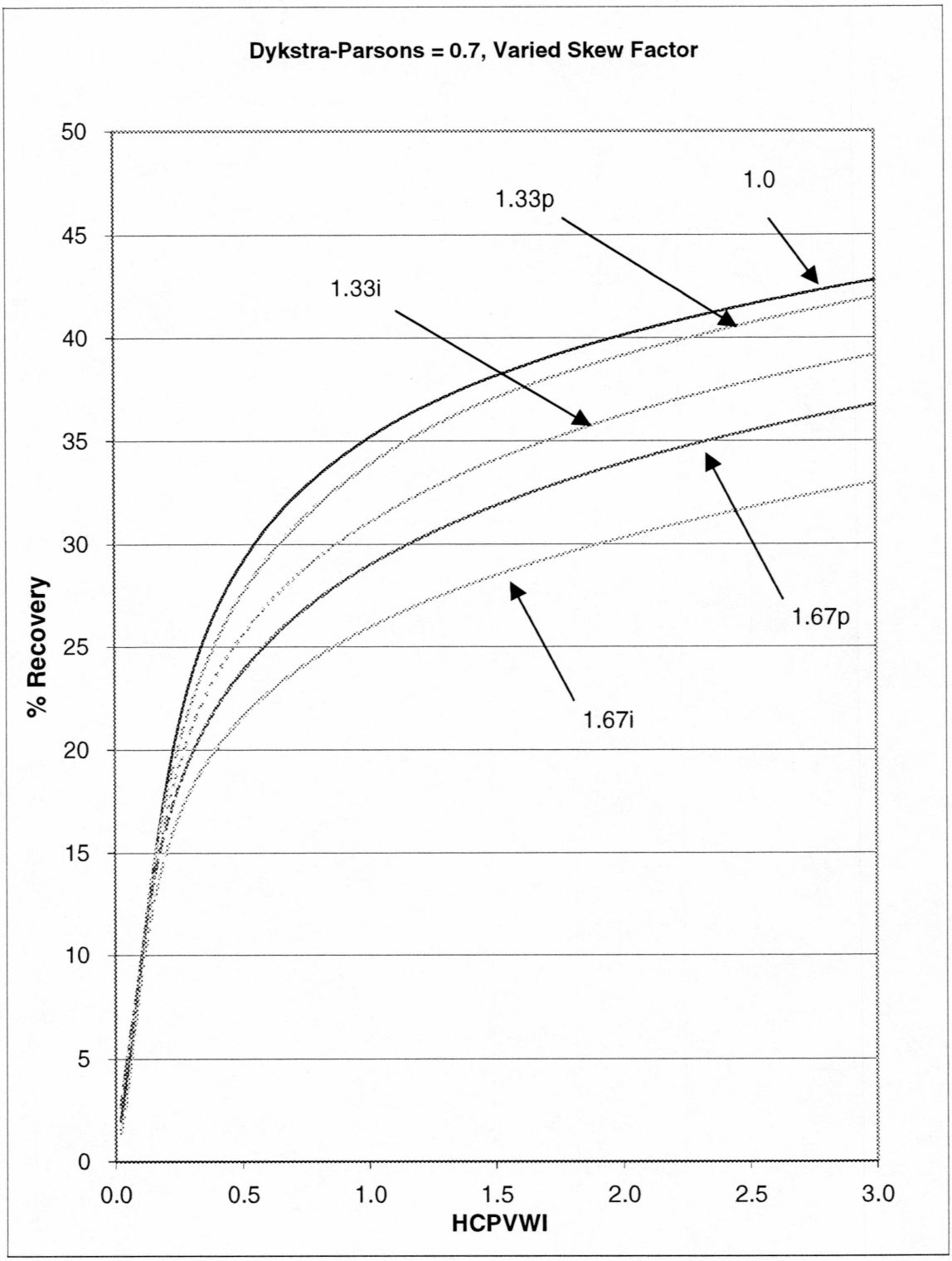

Figure 19: Impact of Skew Factor, Recovery vs. HCPVWI

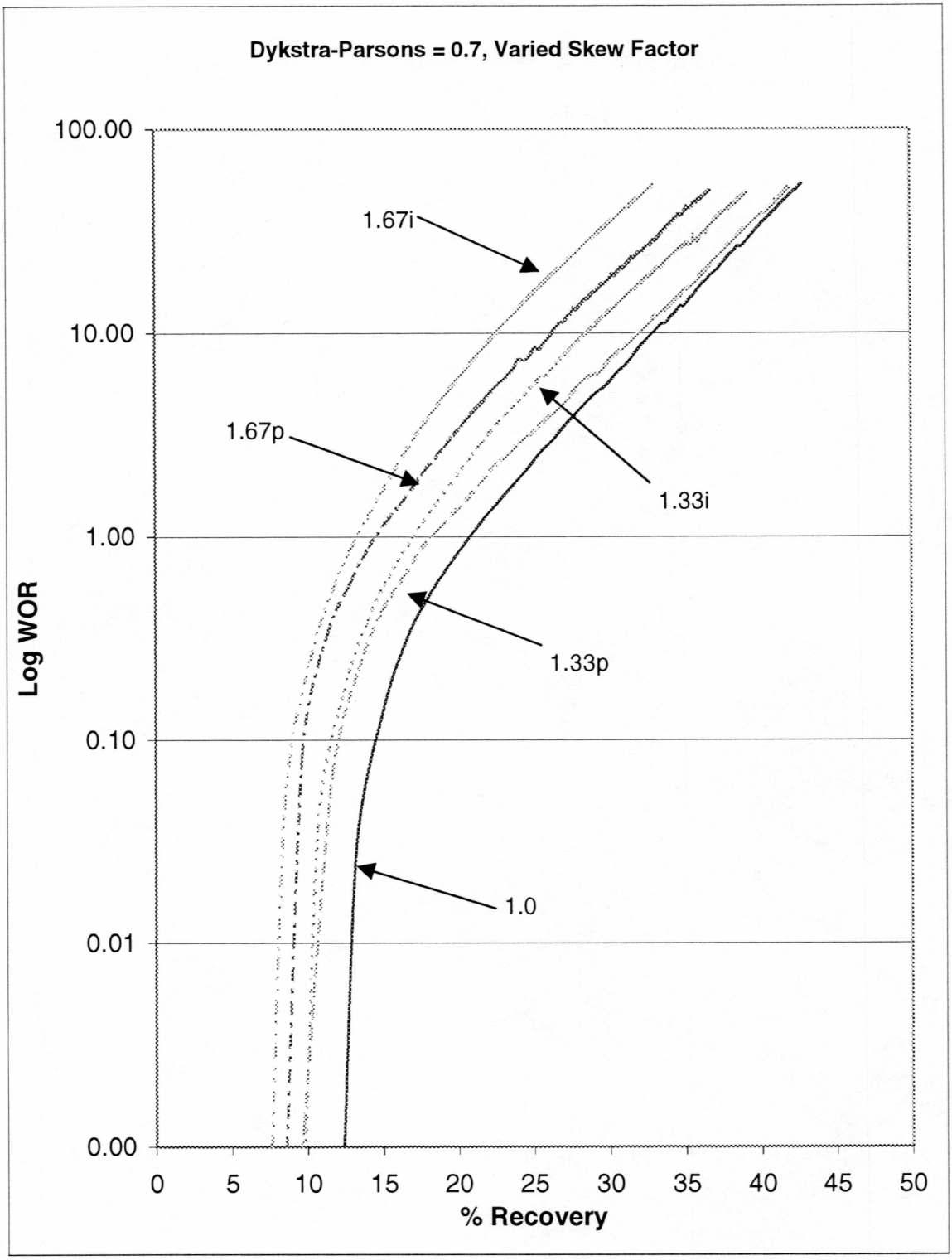

Figure 20: Impact of Skew Factor, Log WOR vs. Recovery